1-1-2010

Power Quality Improvement by Supercapacitor Energy Storage

Irtaza Mohammad Syed
Ryerson University

Power Quality Improvement by Supercapacitor Energy Storage

by

Irtaza Mohammad Syed

B. Eng, NED University of Engineering and Technology

Pakistan, 1996

A thesis

presented to Ryerson University

in partial fulfillment of the

requirements for the degree of

Master of Applied Science

in the Program of

Electrical and Computer Engineering

Toronto, Ontario, Canada, 2010

Author's Declaration

I hereby declare that I am the sole author of this thesis or dissertation.

I authorize Ryerson University to lend this thesis or dissertation to other institutions or individuals for the purpose of scholarly research.

_____

Irtaza M. Syed

I further authorize Ryerson University to reproduce this thesis or dissertation by photocopying or by other means, in total or in part, at the request of other institutions or individuals for the purpose of scholarly research.

_____

Irtaza M. Syed

Borrower's Page

Ryerson University requires the signature of all persons using or photocopying this thesis. Please sign below, provide address and date.

Name	Signature	Address	Date

ABSTRACT

Harnessing green and renewable sources of energy is a future solution that addresses rising energy demands and growing environmental concerns. Among these, tapping wind energy using wind turbines appears to be one of the most promising solutions. A wind energy conversion system captures kinetic energy of wind and converts it into electrical energy.

By nature, availability of wind energy is stochastic and intermittent. In contrast, electric power system expects a steady and planned supply of energy. This thesis addresses the gap in characteristics of wind energy supply and conventional electric energy demand.

This thesis considers a *doubly fed induction generator* (DFIG) connected to a wind turbine to harness wind energy. The proposed topology connects a Supercapacitor through a buck-boost chopper to the DC link of rotor circuit. The Supercapacitor works to perform the job of a flywheel. The thesis proposes an appropriate control system that controls the output of the DFIG to constant value (P_{REF}) eliminating short-term fluctuations. This control system works to control the buck-boost chopper and works as an inner control loop.

Thereafter, this thesis proposes an optimization algorithm that considers short-term forecasted wind speeds (energy) for several minutes. It then optimizes to determine a minimum set of output values of the DFIG (P_{REF}). It ensures that output of the DFIG has minimum changes thus minimizing intermittency in the DFIG output. This optimization algorithm forms the outer loop in the overall control strategy.

The complete system is implemented in Matlab/Simulink and analysed in this thesis. The results demonstrate that the inner and outer control loops work to minimize output power oscillations and improve power quality.

ACKNOWLEDGMENTS

The author expresses his deepest gratitude and appreciation to his supervisors, Professor Dr. Bin Wu and Associate Professor Dr. Bala Venkatesh for their continuous guidance, aspiration, enlightenment, inspiring instruction, encouragement and exceptional support throughout this research.

The financial support represented by the NSERC Discovery grant, Canada awarded to Dr. Bala Venkatesh is gratefully acknowledged.

The author wishes to thank his parents, siblings, family and friends for their support and encouragement.

Finally special thanks to all my instructors, professors and colleagues at Dawood College of Engineering and Technology (NED University) and Ryerson University.

TABLE OF CONTENTS

LIST OF ABBREVIATIONS/ACRONYMS

BESS	Battery Energy Storage System
DFIG	Doubly Fed Induction Generator
ESR	Equivalent Series Resistance
FSFP	Fixed Speed Fixed Pitch
FSVP	Fixed Speed Variable Pitch
GSC	Grid Side Control
IEI	Instantaneous Energy Indicator
IG	Induction Generator
IGBT	Insulated Gate Bipolar Transistor
IST	Iterative Search Technique
kW	kilo Watt
kWh	kilo Watt hour
LAB	Lead Acid Battery
MILPT	Mixed Integer Linear Programming Technique
MPE	Maximum Power Extraction
MPPT	Maximum Power Point Tracking
MW	Mega Watt
MWh	Mega Watt hour
MWs	Mega Watt sec
OCS	Operation Control System
PCS	Power Control System
POA	Power Optimization Algorithm
PQI	Power Quality Improvement
PSS	Pref Setting System
RSC	Rotor Side Control

SC	Supercapacitor
SESS	Supercapacitor Energy Storage System
SLI	System Limits Indicator
SMES	Superconductive Magnetic Energy Storage
TSR	Tip Speed Ratio
VSFP	Variable Speed Fixed Pitch
VSVP	Variable Speed Variable Pitch
WECS	Wind Energy Conversion System
WT	Wind Turbine

LIST OF SYMBOLS

A	Swept area
C_{cell}	Individual cell capacitance
C_{dclink}	DC-link capacitance
C_p	Power co-efficient
C_s	Total series capacitance
C_{sc}	SC capacitance
C_{scmin}	Supercapacitor minimum capacitance
D	Duty cycle
E_{dclink}	Instantaneous energy of DC-link capacitor
E_W	Wind Energy
E_{C0}	SC initial energy
EC_{min}	Minimum SC energy
EC_{max}	Maximum SC energy
E_{ot}	Total output energy in time t
E_{sc}	Energy of SC
ESR_s	Series string resistance
ESR_{cell}	Cell individual ESR
ESR_{sc}	SC-Bank total ESR
EC_0	SC-Bank initial energy
Esc_f	SC-Bank energy at the end of simulation
E_{wt}	Total wind energy in time t
f	Switching frequency of DC-DC converter
f_1	Stator source frequency
f_2	Rotor source frequency
i_{ds}, i_{qs}, i_{dr}, i_{qr}	Stator and rotor d-q axis currents

I_{sc}	SC current
ΔI_L	Change in inductor current
ΔI_{Loff}	Change in inductor current during toff
ΔI_{Lon}	Change in inductor current during ton
L_s, L_r	Stator and rotor inductances
L_m	Magnetizing inductance
n_s	Synchronous speed
n_2	Rotor flux speed due to f_2
n_r	Net rotor speed due to W_T and f_2
n_p	Number of SC series strings needed in parallel to form SC -Bank
n_s	Number of SC cells in series to form SC -Bank
NH	Number of hours
NX	Number of seconds
p	Number of poles
PC	SC power
PC_t	Maximum input in the tth instant
PC_{min}	Minimum SC power
PC_{max}	Maximum SC power
P_m	Mechanical power
P_{meas}	Measured output power of DFIG-WECS
PO_t	Net output power in the tth instant
PO_{max}	Maximum output power
P_r	Rotor power
P_{ref}	Power reference
$P_{ref\text{-}optimal}$	Optimal Pref
P_s	Stator power

P_{sc}	SC-Bank power rating, same WECS Grid Side Converter Rating
P_W	Wind Power
PW_t	Wind power of the tth instant
PW_T	Power extracted by WT
R	Blades radius
R_s and R_r	Stator and rotor resistances
s	Slip
t	Time
t_d	Time of fluctuations that we want to eliminate
t_{off}	Off-time of DC-DC converter
t_{on}	On-time of DC-DC converter
T	Time period of DC-DC converter
T_e	Electromagnetic torque
UD_t	Variable denoting downward Pref level change
US_t	Variable denoting upward Pref level change
V_{cell}	Individual cell voltage
V_{dclink}	DC-link voltage
v_{ds}, v_{qs}, v_{dr}, v_{qr}	Stator and rotor d-q axis voltages
V_{sc}	SC voltage
V_{scmax}	Maximum SC voltage
V_{scmin}	Minimum SC voltage
V_{scnom}	Nominal SC voltage
W	Wind speed
$Wind_{cut\text{-}in}$	Wind cut-in speed
β	Pitch angle
λ	Tip Speed Ratio (TSR)

λ_{ds}, λ_{qs}, λ_{dr}, λ_{qr}	Stator and rotor flux linkages
λ_{opt}	Optimal λ
ρ	Air density
ω_r	Rotor speed
ω_{opt}	Optimal ω_r
ω_s	Synchronous speed

LIST OF TABLES

LIST OF FIGURES

CHAPTER 1

INTRODUCTION

1.1 INTRODUCTION

Electricity from wind energy is one of the fastest growing methods of electricity generation and its penetration in the world is expected to grow up to 12% of the global demand by 2020 [1] . In this type of electricity generation, kinetic energy from moving air is converted into electricity by wind turbines that are mounted in locations where there are favorable weather patterns. Wind turbines may be employed individually, but are often installed in groups to form “wind farms” or “wind power plants”. Electricity generated by wind farms may be used locally or transmitted on the electric grid to power homes and businesses far away. The use of wind energy reduces the environmental impact of generating electricity because it does not require fuel and does not produce pollution or greenhouse gases.

While renewable energy is considered as a key solution to reduce green house gas emissions, its inherent intermittent nature poses a big challenge. One of the problems, besides being non-dispatch-able and others, is associated with the quality of power generated and thus supplied into the grid. These problems become even bigger when wind generators are connected to a weak grid and due to this reason wind power is restricted in some cases. Thus, the problem of intermittency of renewable energy sources cannot be overlooked [2].

1.2 PROBLEM FORMULATION

Quality of power output from wind generators suffer due to sporadic fluctuations of wind speed. This intermittence, an inherent characteristic of wind, imposes special requirements on the surrounding power system. Thus, wind power systems challenge the power quality, energy planning, power flow controls, and dispensability in the local grid. In some cases, it even restricts integration of the wind power.

The horizontal flow of wind consists of two overlapping effects, namely Macro-meteorological and Micro-meteorological fluctuations [3]-[4]. The macro-meteorological fluctuations indicate the movements of large-scale weather patterns such as the day and night cycle, the movement of depressions and cyclones. The micro-meteorological fluctuations originate from the atmospheric turbulence with typical time scales of 1 to 600 seconds. Output of wind generators fluctuate in a similar manner to the wind speeds although they are modified by the physical and electrical characteristics of the wind generator.

Experience and research show that power system is more susceptible and sensitive to medium frequency wind power fluctuations (0.01 ~ 1 Hz) [5]-[6]. Integration of an energy storage system into a wind generator can effectively suppress these power fluctuations and thus improve quality of power supplied to the connected grid. Smoothing long-term power fluctuations requires a higher capacity of storage and thus a higher cost. The cost of this solution is the main limiting factor in its application.

A short term energy storage solution presents itself as the optimal solution to the problem of short term fluctuations (1 – 600 sec) [3]-[4] from size, cost and quality point of view. A variety

of options is available but different factors dictate a choice of Supercapacitor (SC) as an Energy Storage device. Supercapacitor Energy Storage Systems (SESS) are used to reduce voltage flicker, current harmonic elimination, compensation of pulsating load and uninterruptable power supply[7]-[10], but less is done in the field of wind energy[11],[12]. Superconducting Magnetic Energy Storage (SMES) System and Battery Energy Storage System (BESS) have been researched on short term wind power fluctuations smoothing [13], but SESS with less auxiliary equipment is more stable and convenient than SMES and it has longer cycle life and less maintenance compared to BESS.

This research thesis focuses on decoupled control of short term power fluctuations with SESS and two quadrant DC-DC converter with an output power optimization algorithm for Doubly Fed Induction Generator (DFIG) based Wind Energy Conversion Systems (WECS). The proposed topology is shown in Figure 1 and verified by simulation in Matlab/Simulink.

DFIG-WECS is shown in solid while the proposed topology is shown in shaded and dotted lines. The proposed topology consist of SC-Bank (Energy storage) connected to DFIG-WECS through a DC-DC (Buck-Boost) converter. DC-DC converter is controlled through a proposed control scheme to either extract power from or inject power into the DFIG-WECS based on the optimal power reference set by Power Optimization Algorithm (POA).

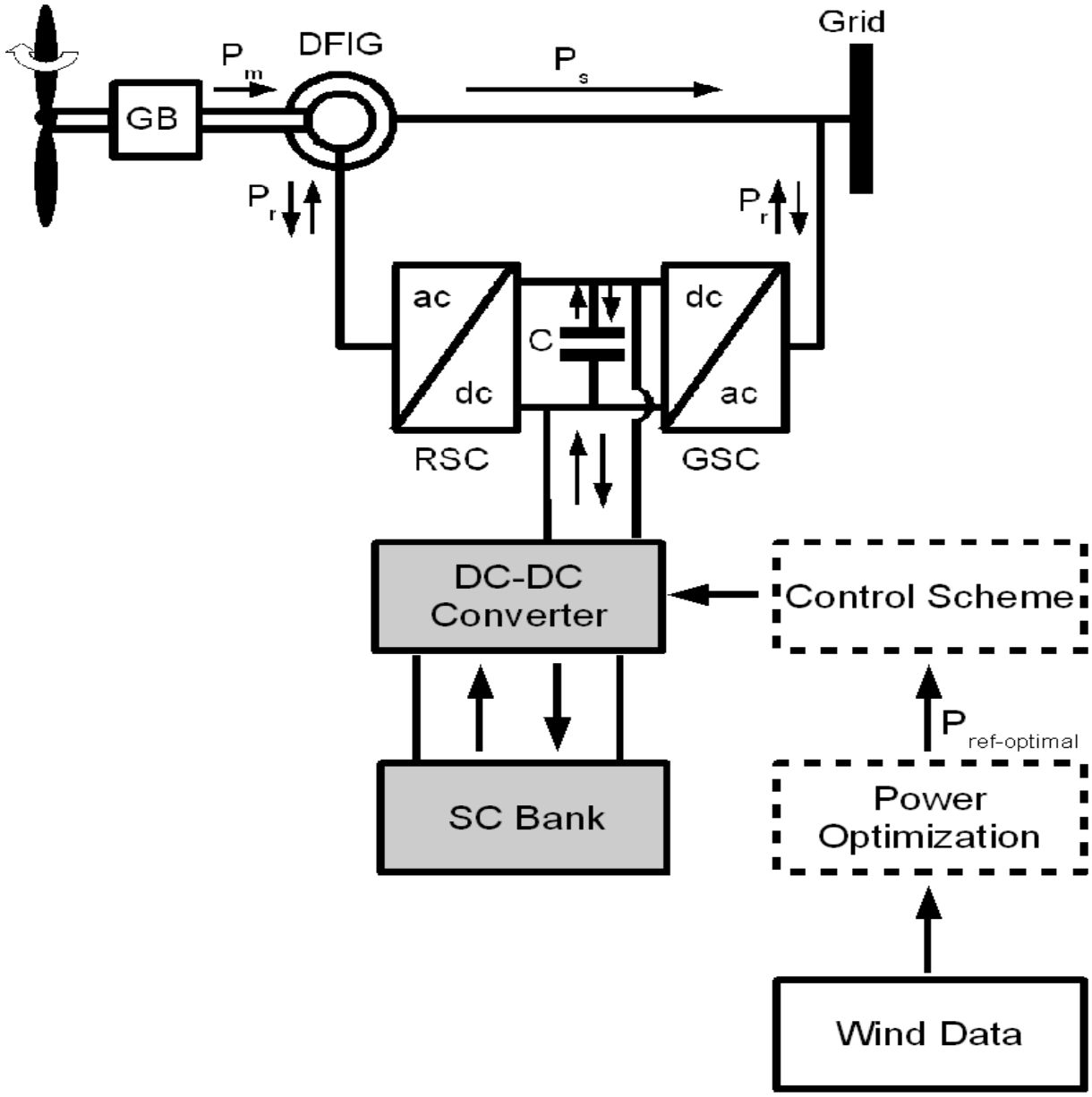

Figure 1: DFIG-WECS with proposed topology (dotted line and shaded boxes)

This thesis is organized in the following manner. Chapter 2 provides the basic system being optimized and proposes the use of SESS connected to a DFIG using a chopper. Chapter 3 presents the proposed control algorithm for ensuring that the DFIG outputs a set value of power. It forms the inner control loop. Chapter 4 shows results of simulation for DFIG-WECS both with and without the proposed topology and the proposed inner control algorithm. Chapter 5 proposes two power optimization algorithms and their solution methods that consider a forecasted wind generation and determine the optimal output such that the output is as steady as possible. These optimization algorithms form the outer control loop. The results of this study are discussed. Chapter 6 presents conclusions for the thesis.

CHAPTER 2

WIND ENERGY CONVERSION SYSTEM

2.1 INTRODUCTION

A wind energy conversion system is a complex system in which knowledge from a wide array of fields comprising Aerodynamics, Mechanical, Civil and Electrical Engineering come together. The principle components of a modern wind turbine are the tower, the rotor and the nacelle, which accommodates the transmission mechanisms and the generator as shown in Figure 2 [21]. The wind turbine captures wind's kinetic energy in the rotor consisting of two or more blades mechanically coupled to an electrical generator. The main component of the mechanical assembly is the gearbox, which transforms the slower rotational speeds of the wind turbine to higher rotational speeds on the electrical generator side. The rotation of the electrical generator's shaft driven by the wind turbine generates electricity, whose output is maintained as per specifications, by employing suitable control and supervising techniques. Besides monitoring the output, these control systems also include protection systems to protect the overall system.

WECS can either operate at a fixed speed or a range of speeds with a fixed or a variable pitch. Both Synchronous and Induction machines can be employed in WECS. WECS can be employed in isolated grids, on-grid or off-grid applications. Each type of WECS and method of deployment has its own set of advantages and disadvantages.

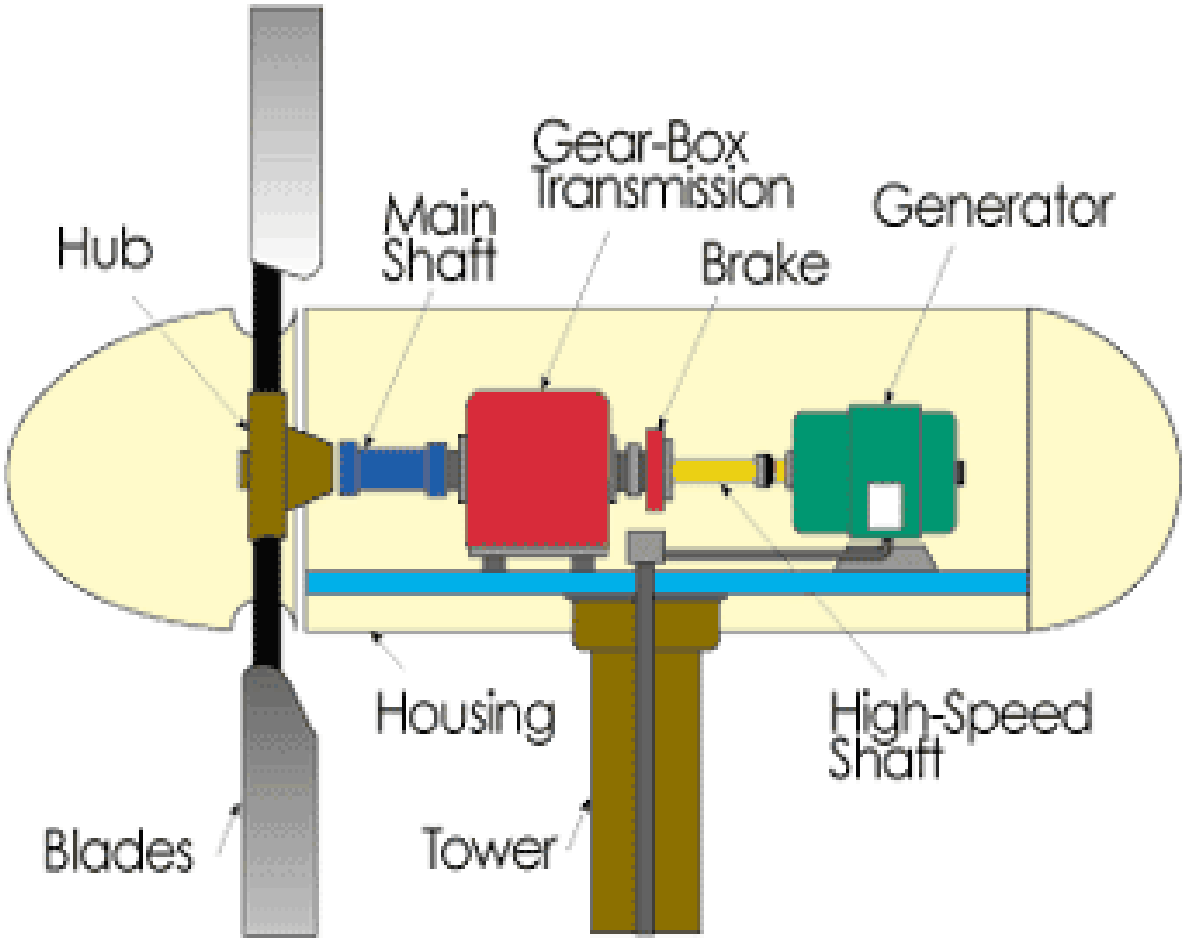

Figure 2: Wind Turbine [21]

Wind Energy Conversion System (WECS) is used to capture the energy available in the wind to convert into electrical energy.

Energy available in wind is given by

$$E_W = \frac{1}{2} \rho A W^3 t \quad (1)$$

where E_W is wind Energy, ρ is air density, A is swept area, W is wind speed and t is time.

Instantaneous Power can be computed by:

$$P_W = \frac{1}{2} \rho A W^3 \quad (2)$$

where P_W is a wind Power.

Wind power extracted by Wind Turbine (WT) depends on C_p, given by

$$C_p = P_{WT} / P_W \quad (3)$$

where C_p is power co-efficient and $C_p \leq 59\%$, known as Betz limit [20].

Combining (2) & (3)

$$P_{WT} = \frac{1}{2} \rho A W^3 C_p \quad (4)$$

where P_{WT} is power extracted by WT.

C_p is not a constant and is the function of (λ, β), where λ is Tip Speed Ratio (TSR) and β is the pitch angle. Tip Speed Ratio (TSR) is given by

$$\lambda = \omega_r . R/ W \quad (5)$$

where R is wind turbine radius and ω_r is generators rotor speed.

Consequently, from (4) & (5), for Maximum Power Point Tracking (MPPT) for all wind speeds we need optimal values of λ & β for every wind speed. It is obvious then that for MPPT we need a Wind Energy Conversion System (WECS) that allows changes in λ & β as W changes. Now as

every $C_{p,\ optimal}$ has only one optimal value of $\lambda_{optimal}$, therefore it is important to achieve this $\lambda_{optimal}$ for every wind speed (W) by controlling rotor speed. Achieving this $\lambda_{optimal}$ for every wind speed (W) ensures maximum power extraction for every W and this process is known as Maximum Power Point Tracking (MPPT) and given by

$$PW_t = \tfrac{1}{2}\rho A(R\ \omega_{opt}/\lambda_{opt})^3\ C_p \qquad (6)$$

where PW_t is optimal value of P_{WT}, ω_{opt} is optimal ω_r and λ_{opt} is optimal λ.

2.2 WECS TYPES

Fixed speed WECS are divided into Fixed Speed Fixed Pitch (FSFP) and Fixed Speed Variable Pitch (FSVP).

In FSFP, Induction Generator (IG) is directly connected to the Grid, IG speed is locked to grid frequency and maximum conversion is possible at only one wind speed (W).

In FSVP, IG is directly connected to the Grid, IG speed is locked to grid frequency and maximum conversion is possible at only one W but also performs better at low wind speed due to variable pitch.

Variable speed WECS are divided into Variable Speed Fixed Pitch (VSFP) and Variable Speed Variable Pitch (VSVP).

In VSFP, IG is connected to the Grid through power converter, IG speed is not locked to grid frequency and maximum conversion is possible at more than one W but no pitch regulation.

In VSVP, IG is connected to the Grid through power converter, IG speed is not locked to grid

frequency and maximum conversion is possible at more than one W additionally provides pitch regulation.

In this work we chose VSVP, which employs a DFIG, based on the reasons outlined below:

- Enhanced energy capture in a wide range wind speeds
- Ability to control active and reactive power
- Reduced size of power electronics converter (rated at 30% of power generated)
- Less power losses (due to reduced size power converter)
- Improved power quality (reduced tower and flicker effects)
- Reduced stresses of the mechanical structure
- Reduced acoustic noise
- Cost effective

Due to these same reasons, most of the major wind turbine manufactures are developing new wind turbines based on variable-speed operation with pitch control using a direct-driven synchronous generator and DFIG. Therefore, DFIG is the best candidate for larger wind turbines.

2.3 DOUBLY FED INDUCTION GENERATOR WECS

Doubly fed induction generator (DFIG) is modeled using "SimPowerSystems" blockset [ver. 7.3.0.324] and implements the well-known Park transformation induction machine model in a stationary reference frame, shown in Figure 3 [23].

Voltage equations are:

$$v_{ds} = R_s i_{ds} + p\lambda_{ds} \quad (7)$$

$$v_{qs} = R_s i_{qs} + \frac{d\lambda_{qs}}{dt} \quad (8)$$

$$v_{dr} = R_r i_{dr} + \frac{d\lambda_{dr}}{dt} + \omega_r . \frac{d\lambda_{dr}}{dt} \quad (9)$$

$$v_{qr} = R_r . i_{qr} + p . \frac{d\lambda_{qr}}{dt} - \omega_r . \frac{d\lambda_{qr}}{dt} \quad (10)$$

where v_{ds}, v_{qs}, v_{dr}, v_{qr} are stator and rotor d-q axis voltages, i_{ds}, i_{qs}, i_{dr}, i_{qr} are stator and rotor d-q axis currents, R_s and R_r are stator and rotor resistances, ω_r is rotor speed and λ_{ds}, λ_{qs}, λ_{dr}, λ_{qr} are stator and rotor flux linkages.

Flux linkage equations are:

$$\lambda_{ds} = L_s i_{ds} + L_m i_{dr} \quad (11)$$

$$\lambda_{qs} = L_s i_{qs} + L_m i_{qr} \quad (12)$$

$$\lambda_{dr} = L_r i_{dr} + L_m i_{ds} \quad (13)$$

$$\lambda_{qr} = L_r i_{qr} + L_m i_{qs} \quad (14)$$

where $L_s = L_{ls} + L_m$ and $L_r = L_{lr} + L_m$ and L_s, L_r are stator and rotor inductances, L_m is magnetizing inductance.

Torque equation is:

$$T_e = 3p/2\ (i_{qs}\lambda_{ds} + i_{ds}\lambda_{qs}) \quad (15)$$

where T_e is electromagnetic torque and p is number of poles.

DFIG is a Wound Rotor Induction Machine (WRIM) with stator and rotor connected to different sources, thus doubly fed. Usually stator is directly connected to the grid with a fixed frequency and rotor via frequency converter. The method which involves additional voltage of variable frequency in the rotor winding, based on the fact that for electromechanical power conversion

magnetic fields generated by stator and rotor currents must be mutually static, i-e they have to rotate with same speed.

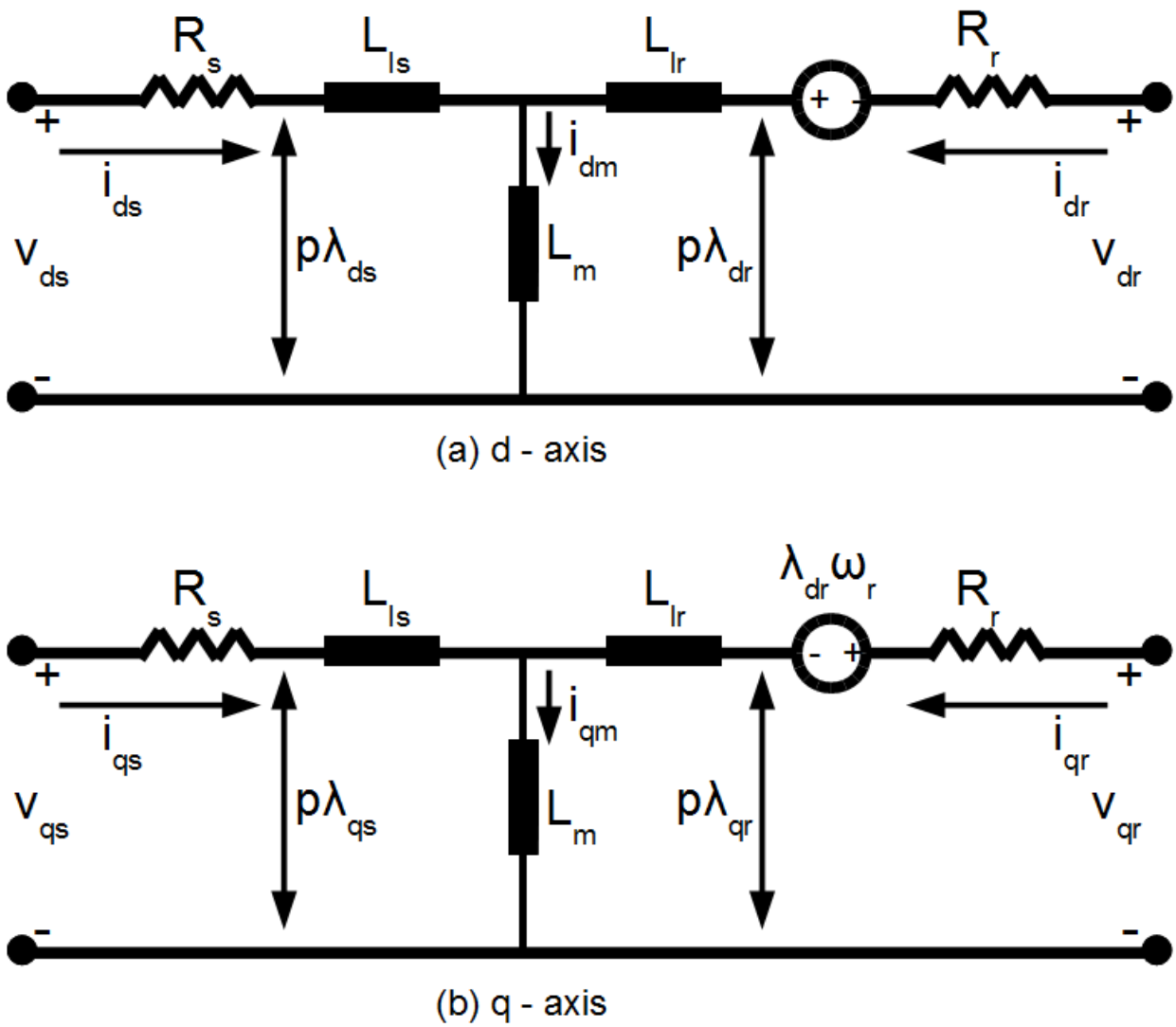

Figure 3: Stationary reference frame model [23]

Consider a machine with a stator having p poles that is connected to a source with a frequency of f_1 and a shorted rotor terminals. The flux created by the stator will rotate at synchronous speed given by [19]

$$n_s = \frac{120}{p} f_1 \tag{16}$$

Now if the rotor is connected to an electrical source of frequency f_2, then there will be a flux created by the rotor that will rotate at a speed with respect to the rotor given by [19]

$$n_2 = \frac{120}{p} f_2 \tag{17}$$

Since the two magnetic fields, due to stator and rotor, must rotate synchronously, therefore

$$n_s = n_r + n_2 \tag{18}$$

Using (16), (17) and re-arranging (18) can be

$$n_r = \frac{120}{p}(f_1 - f_2) \tag{19}$$

If any two phases of the source connected across the rotor are interchanged then [19]

$$n_r = \frac{120}{p}(f_1 + f_2) \tag{20}$$

In general, the rotor's mechanical speed of a DFIG machine is given by [19]

$$n_r = \frac{120}{p}(f_1 \pm f_2) \tag{21}$$

As shown in the Figure 4, a DFIG can be operated in sub-synchronous or super-synchronous modes as determined by the phase sequence of the voltage. A range of ± 30% of rated speed is achieved by varying the magnitude and frequency of the voltage applied across the rotor. Positive phase sequence rotor voltage results in the sub-synchronous mode and a negative phase sequence rotor voltage results in the super-synchronous mode of operation.

As shown in the Figure 5, the DFIG stator is directly connected to grid while rotor is connected to grid through Rotor Side Converter (RSC) and Grid Side Converter (GSC) with DC-link capacitor between them for decoupled control. Both RSC and GSC are voltage source converters that use forced-commutated power electronic devices (IGBTs) to synthesize an AC voltage from a DC voltage across the DC-link capacitor. Sometimes a transformer is used to connect GSC to the grid, as well. The three phase rotor windings are connected to RSC by slip rings and brushes. The power extracted by the Wind Turbine is converted into electrical power by induction generator and transmitted to grid by both rotor and stator. The control system generates the pitch angle command and the voltage command signals V_r and V_g for RSC and GSC respectively, in order to control power of the wind turbine, the DC bus voltage and the reactive power or voltage at the grid terminals.

In this arrangement, the stator always delivers power to the grid but direction of the rotor power depends on the mechanical speed of the rotor. The rotor power flows into the grid for super-synchronous speeds and the rotor draws power from the grid for sub synchronous mode. At the synchronous speed, rotor does not draw or supply power to the grid. The rotor power supplied to grid at super-synchronous speed tends to increase DC-link voltage and vice-versa at sub synchronous speed. GSC is thus used to keep this voltage constant. The phase sequence of the AC voltage generated by the RSC constitutes a positive-sequence for the sub synchronous speed and negative for super synchronous speed. Both RSC and GSC can be used to absorb or generate reactive power or control voltage at the grid terminals but RSC is preferred due to the reduction

in converter rating requirement as reactive power injection through the rotor is effectively amplified by a factor of 1/s, where s is slip.

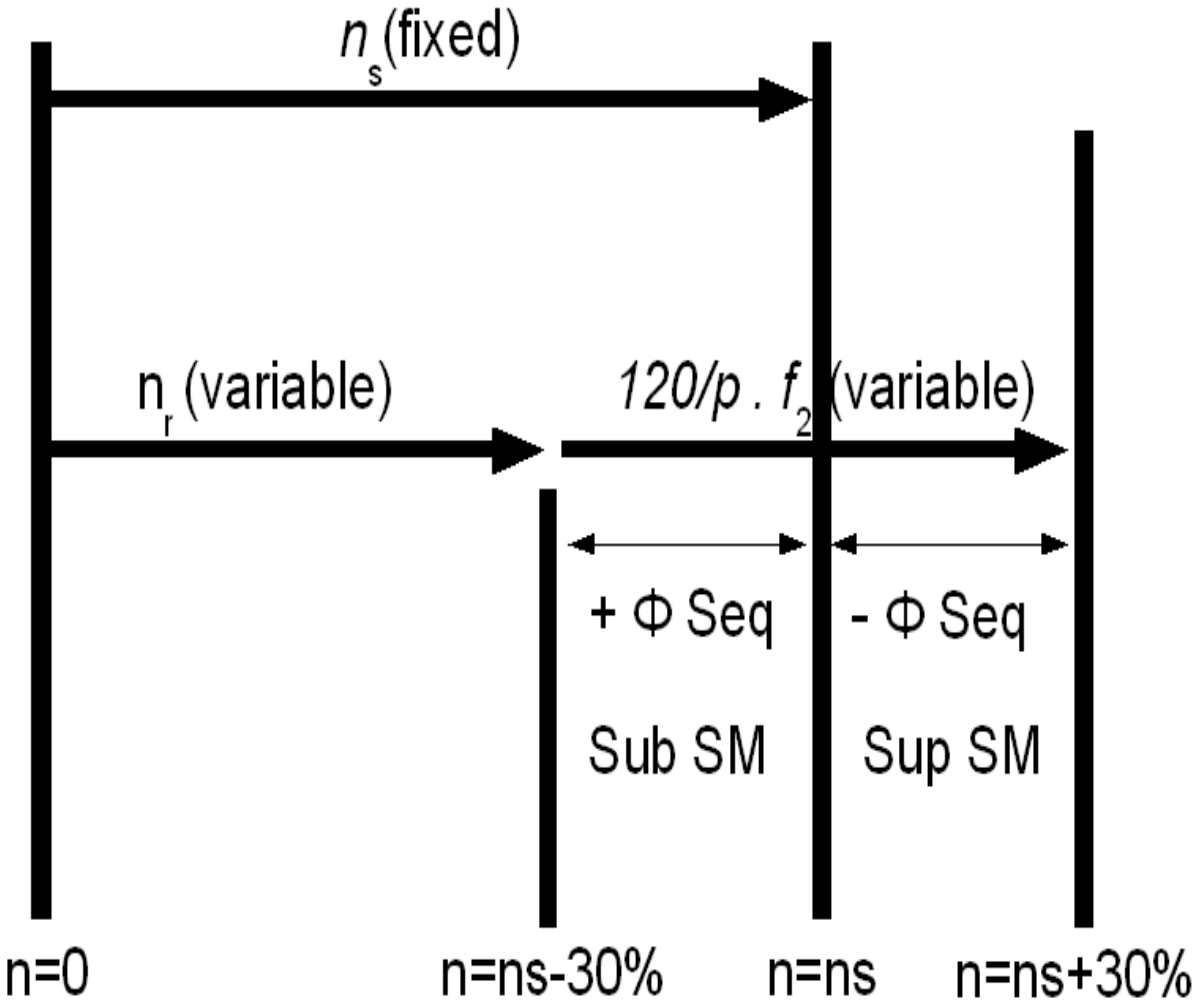

Figure 4: DFIG Speed-frequency relationship

The generator control is based on dq control coordinate system, where the q-axis component is used to control active power and d-axis component is used to control reactive power. The dq coordinate system decouples the speed control action from the reactive power and/or voltage control. This allows the two rotor voltages V_{dr} and V_{qr} to be regulated separately. DFIG control system performs the following [22]:

- For speeds less than or equal to rated speed, pitch angle is kept constant at zero and for speeds higher than rated speed pitch angle is changed in such a way that power is kept constant at rated value despite of changes in wind speed (Pitch angle control).
- Power flow control such that a pre-defined power-vs-speed characteristic is followed and also absorbs /generates reactive power or control voltage at the grid (RSC control).
- Keeping DC-link voltage constant by transferring real power from/to DC-link capacitor (GSC control).

The relationships among different parameters for DFIG operating in steady state with ideal characteristics (neglecting losses) as shown in Figure 5 are [20]:

$$P_s = P_m - P_r \tag{22}$$

where P_s is Stator power, P_m is mechanical power and P_r is rotor power.

$$T_e = P_m / \omega_r \tag{23}$$

where T_e is torque and ω_r is rotor speed.

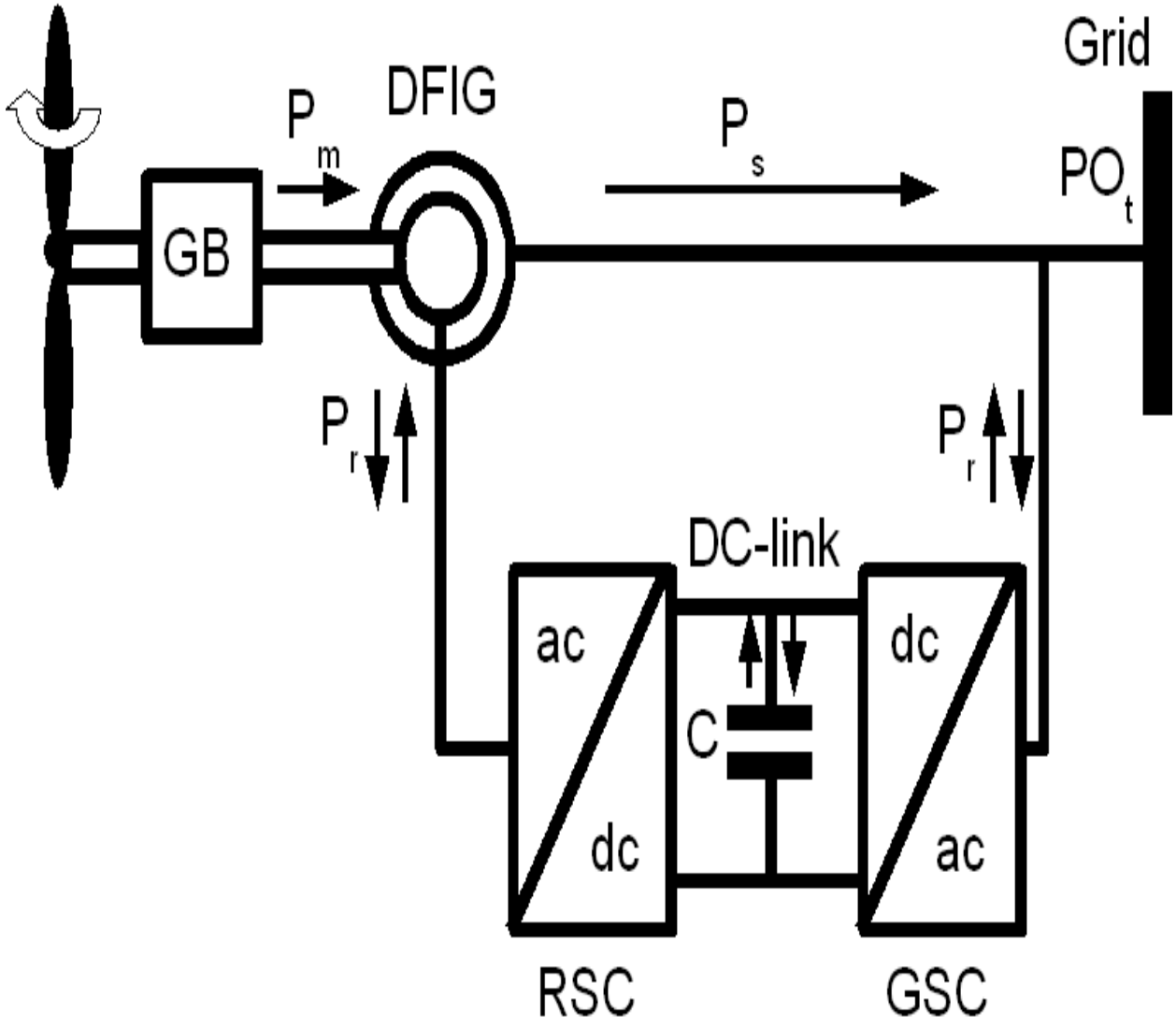

Figure 5: DFIG-WECS (Lossless)

$$s = (\omega_s - \omega_r)/ \omega_s \quad (24)$$

where ω_s is a synchronous speed, ω_r is a rotor speed and s is slip. Slip (s) denotes the speed difference between the rotor speed and the synchronous speed, usually expressed as a percent of the synchronous speed .

Rotor power is related to stator power by slip and is given as

$$P_r = -s\, P_s \quad (25)$$

Using (22) and (25)

$$P_m = (1 - s)\, P_s \quad (26)$$

Therefore

$$PO_t = P_s + P_r \quad (27)$$

where PO_t is the power supplied into the grid.

CHAPTER 3

POWER QUALITY IMPROVEMENT BY SUPERCAPACITOR ENERGY STORAGE SYSTEM

3.1 INTRODUCTION

Proposed system as shown in Figure 6 consists of DC-DC converter, SC-Bank, Control Scheme and Power Optimization Algorithm. The operating principle can be outlined as:

- The instantaneous value of $P_{ref\text{-}optimal}$ is defined by Power Optimization Algorithm (Chapter 5) for a given wind data set using a proposed optimization algorithm.
- Control scheme block
    - The control scheme aims to hold DFIG's output PO_t equal to $P_{ref\text{-}optimal}$
    - Compares output power PO_t with $P_{ref\text{-}optimal}$
    - Controls DC-DC converter to either work in Buck or Boost mode to extract or inject power so that PO_t becomes equal to $P_{ref\text{-}optimal}$
    - SC-Bank either works as storage or source of energy

This chapter presents the DC-DC converter, SC-Bank and Control scheme (the inner control loop). The Power Optimization Algorithm (POA) will be discussed in Chapter 5.

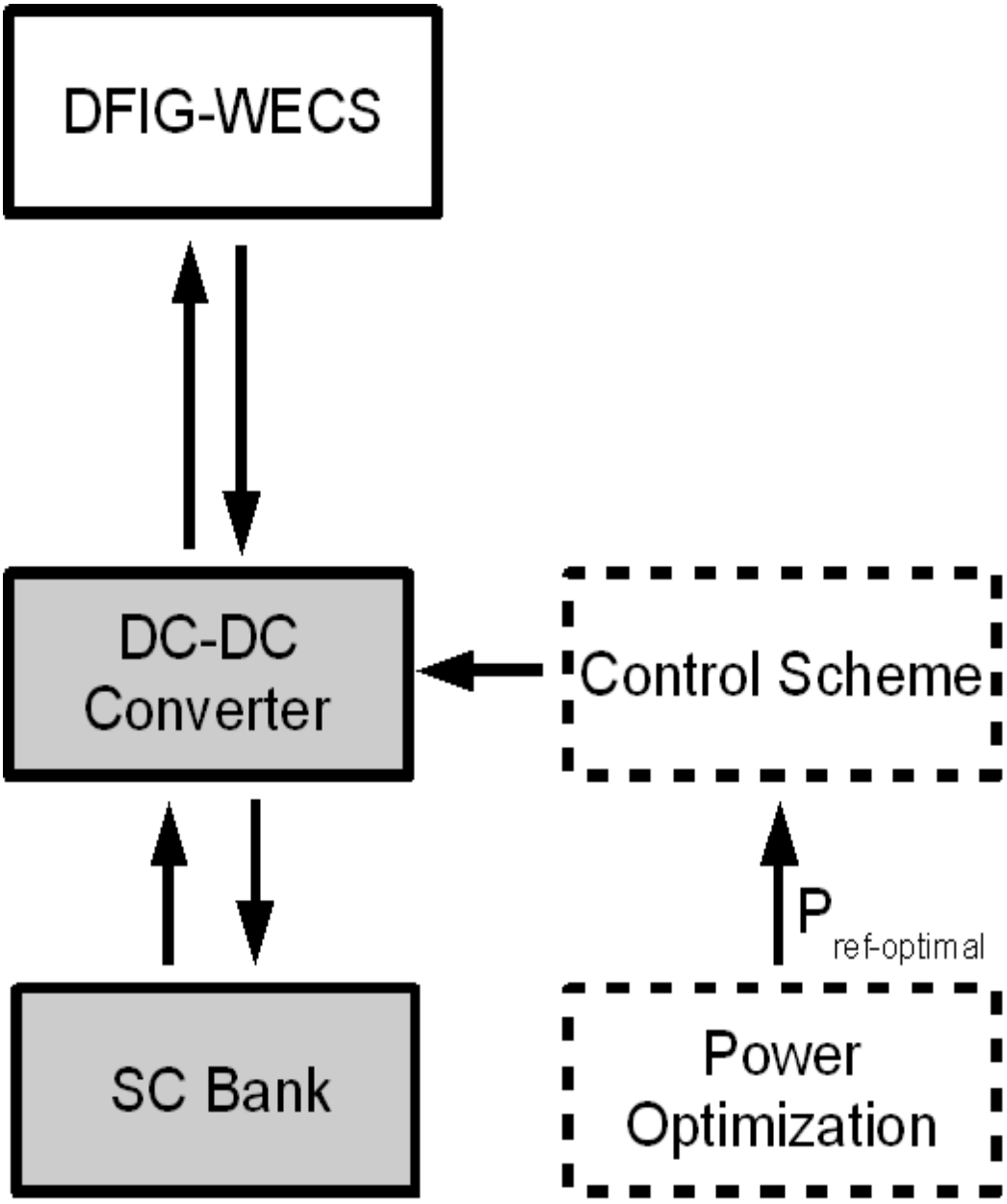

Figure 6: Proposed topology (dotted and shaded)

3.2 SUPERCAPACITOR

The concept and usage of capacitors is not new, however supercapacitor (SC) with low Equivalent Series Resistance (ESR) is a relatively new technology. SC with high ESR, suitable for low current applications, has existed for some time now; the breakthrough in the technology is the SC with low ESR. In this work, we consider SC with low ESR. In terms of power, SC power density supersedes both capacitor and battery but in terms of energy density, SC is better than capacitors but lags behind batteries.

Supercapacitors are different from other capacitors in terms of the electrodes used. Supercapacitors are based on a carbon (nanotube) technology [26]. The carbon technology used in these capacitors creates a very large surface area with an extremely small separation distance by a physical barrier made from activated carbon that when an electrical charge is applied to the material a double electric field is generated which acts like a dielectric. The thickness of the electric double layer is as thin as a molecule. The surface area of the activated carbon layer is extremely large yielding several thousands of square meters per gram. This large surface area allows for higher power densities.

SC model used in this study is shown in Figure 7 and is adequate for this kind of study [17]. A selection criterion for storage systems is usually based on: Storage capacity, Available power, Depth of discharge or Power transmission rate, Charge / Discharge time, Efficiency, Durability (cycling capacity), Costs, Feasibility, Self-discharge, Mass and volume densities of energy, Monitoring and control equipment, Operational constraints, Reliability, Ease of maintenance, Simple design, Operational flexibility and Environmental aspects [14].

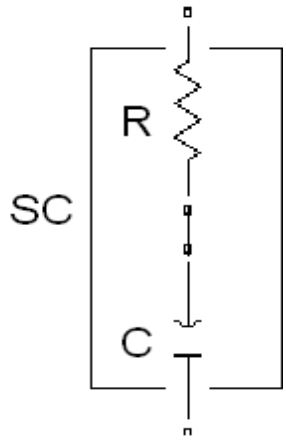

Figure 7: SC model

SC as a storage device was chosen by comparing characteristics of Lead Acid Battery (LAB) and SC as given in the Table 1. Energy related cost ($/kWh) of LAB is $245 per kWh and supercapacitor is $82,000 per kWh while power related cost ($/kW) for LAB is $300 per kW and $300 per kW for supercapacitor [25]. It may be summarized that, from Table 1, for fast charge/discharge applications such as this, SC is highly desirable.

The maximum voltage across a single cell of Supercapacitor is in the range of 2.7 V to 3.0 V. A combination of Supercapacitor cells are required to create the SC-bank with design objectives such as maximum SC-Bank voltage (V_{scmax}), minimum SC-Bank voltage (V_{scmin}), nominal SC-Bank voltage (V_{scnom}), SC-Bank current (I_{sc}), Supercapacitor power rating (P_{sc}), discharge time (t_d), individual SC cell capacitance (C_{cell}) and individual SC cell voltage (V_{cell}).

Table 1: Characteristics of SC and Lead Acid Battery (LAB) [12] [15] [16]

Feature	SC	LAB
High power density	Yes	No
High efficiency of cycles	Yes	No
Long cycle life	Yes	No
Long shelf life	Yes	No
Shorter dis/charge time	Yes	No
Wider temperature range	Yes	No
Easy to charge	Yes	No
Low internal resistance	Yes	No
Environmentally safe	Yes	No
No maintenance	Yes	No
High energy density	No	Yes
Slow self discharge	No	Yes
Low price	No	Yes

Now connecting these cells in series and parallel combination forms a bank. The combination affects the ESR and capacitance of the SC-bank. The following procedure is used to find how many parallel strings of series connected Supercapacitor cells are needed and with how many Supercapacitor cells are required in each series string. Consider the rated voltage of a Supercapacitor cell as V_{cell} then the total voltage of the SC-Bank equals:

$$V_{scmax} = n_s \cdot V_{cell} \tag{28}$$

Similarly if the Equivalent Series Resistance of a cell is ESR_{cell} then the series string ESR is:

$$ESR_s = n_s \cdot ESR_{cell} \tag{29}$$

where n_s is number of SC cells in series to form a single string. Individual series string capacitance (C_s) of n_s series SC cells is given by

$$C_s = C_{cell} / n_s \tag{30}$$

Considering the power rating of the SC-bank (P_{sc}) and a minimum SC-bank voltage of V_{scmin}, the maximum current (I_{scmax}) received by the SC-Bank is given by

$$I_{scmax} = P_{sc} / V_{scmin} \tag{31}$$

Now as current (I_{cell}) of an individual series string with n_s series SC cells is less than I_{scmax}, we need n_p number of series strings in parallel to form the SC-Bank, given by

$$n_p = I_{scmax} / I_{cell} \tag{32}$$

Now total capacitance (C_{sc}) due to n_p number of series strings in parallel is given by

$$C_{sc} = n_p C_s \tag{33}$$

Finally, the total ESR (ESR_{sc}) due to n_p number of series strings in parallel is given by

$$ESR_{sc} = ESR_s / n_p \tag{34}$$

Figure 8 shows such an arrangement to from a SC-Bank.

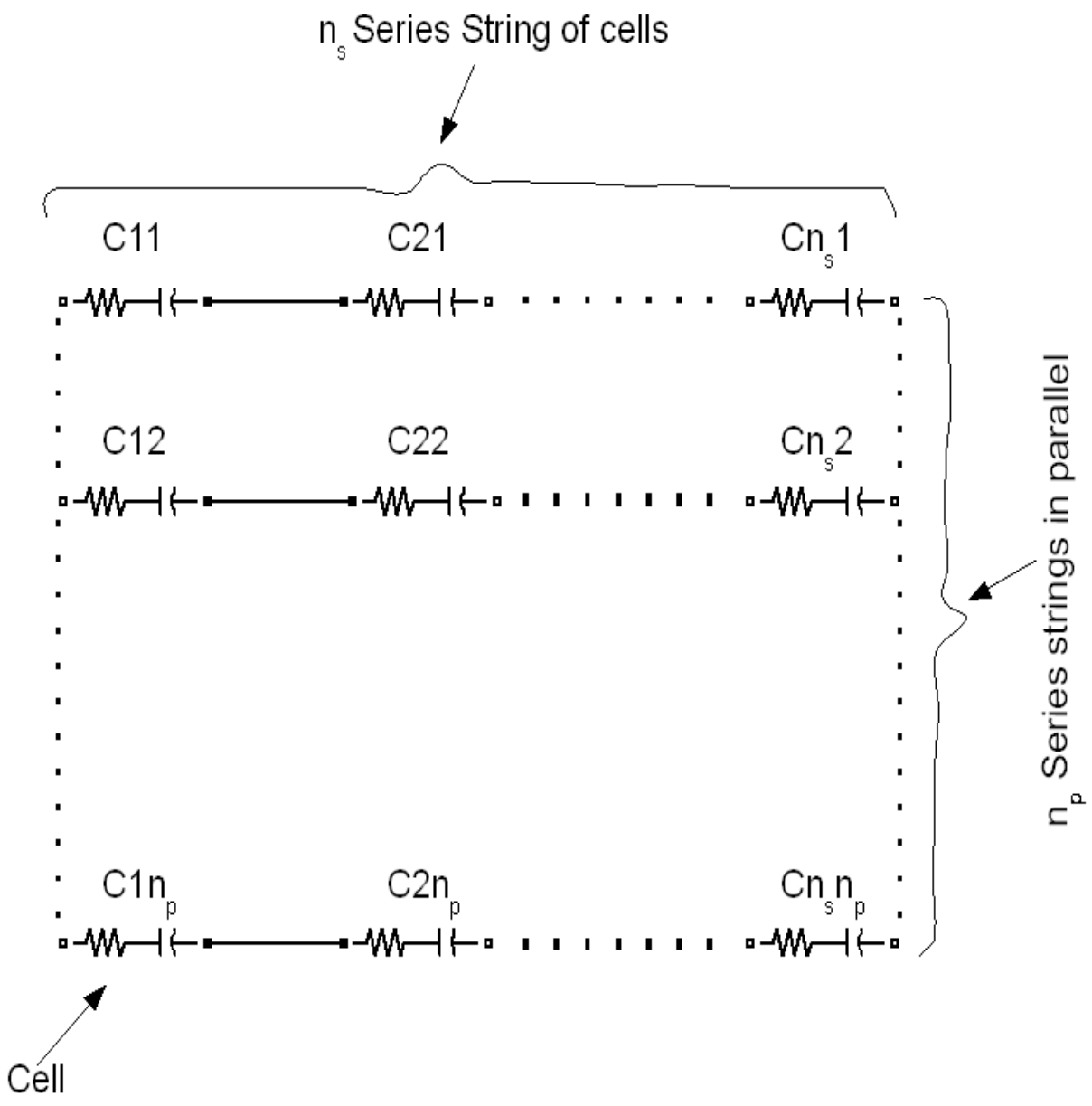

Figure 8: SC-Bank

3.3 DC/DC CONVERTER

A DC-DC converter, shown in Figure 6 at the beginning of this chapter and proposed in this study, is a 2-quadrant buck-boost chopper. Figure 9 shows Buck-Boost converter with DC-link capacitor added to a converter on one side and SC on the other side. The two-quadrant chopper is made to switch between Buck and Boost modes as the need arises and thus ensures flow of current in both directions with a fixed voltage polarity. It operates in the Boost mode when transferring power from SC to DFIG-WECS and in the Buck mode while transferring power in the other direction to keep DC-link voltage constant, simply by varying duty cycle.

As electronic devices inherently carry current in one direction therefore anti-parallel diodes are included to get bi-directionality. The SC voltage is limited to a lower voltage (V_{scmin}) of 100 volts to avoid the Supercapacitor voltage (V_{sc}) dropping to zero volts and thus preserve stability and efficiency of the buck-boost converter.

3.3.1 SIZING OF THE INDUCTOR

In boost mode, IGBT2 is turned on (with IGBT1 turned off) and thus inductor energy builds up linearly assuming that the SC behaves as a DC source and the inductor (L) is ideal. The change in the inductor's current is given by

$$\Delta I_{L\text{-}on} = (V_{sc}/L)\, t_{on} \tag{35}$$

where $\Delta I_{L\text{-}on}$ is a change in inductor current for on-time, t_{on}. When IGBT2 is turned off (with IGBT1 turned ON) then inductor energy decays linearly and is given by

$$\Delta I_{L\text{-}off} = [(V_{sc} - V_{dclink})/L]\, t_{off} \tag{36}$$

where $\Delta I_{L\text{-}off}$ is a change in inductor current for off-time, t_{off} and V_{dclink} is DC-link voltage.

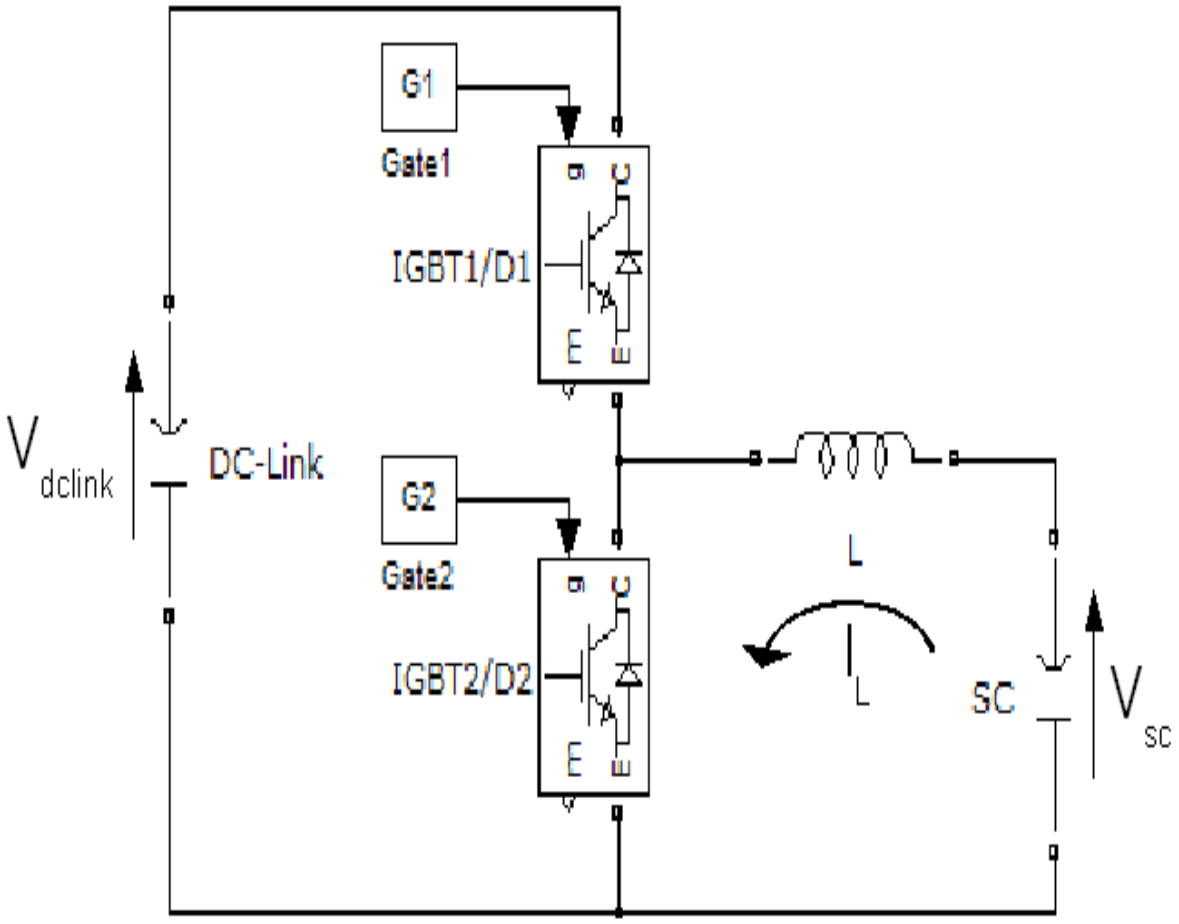

Figure 9: 2 Q chopper with SC & DC-link Cap

But the DC-link voltage is given by (32), the standard boost converter equation [24]

$V_{dclink} = V_{sc} /(1-D)$ (37)

where D is duty cycle and given as

$D= t_{on}/T$ (38)

Therefore

$\Delta I_{L-off} = [(V_{sc}- V_{sc} /(1-D))/L]\ t_{off}$ (39)

Choosing a 50% duty cycle ($t_{off} = t_{on}$) for design purposes and using $\Delta I_L = \Delta I_{L-off} = \Delta I_{L-on}$, equation (35) becomes

$L = (V_{sc}/ \Delta I_L)\ D\ .\ T$ (40)

where T is period and *f* is switching frequency.

The DFIG-WECS chosen in this study has the following data: DC-link voltage is 1200 volts, Grid Side Converter rating is 0.75 MW and a switching frequency of 1620 Hz. The Grid Side Converter rating of 0.75 MW is chosen to equal the Supercapacitor rating, P_{sc}. In the proposed topology, the SC-Bank is designed for a maximum voltage of 1350 volts (V_{scmax}), a minimum voltage of 100 volts (V_{scmin}) and a nominal operating voltage of 1200 volts (V_{scnom}, DC-link voltage). Thus, the minimum inductance required for the buck-boost converter (L) is calculated with the following data:

P_{sc}= 0.75 MW, V_{scnom} = 1200 V, V_{scmax} = 1350 V, V_{scmin} = 100 V, *f* = 1620 Hz, D = D_{max} =1 (to allow for maximum ripple), and with a ripple of 1%.

The maximum SC-bank current is:

$I_{scmax} = P_{sc} / V_{scmin} = 7.5$ kA

Now inductor current ripple allowed of 1% is

ΔI_L =75 A

Then value of inductor is

$L = (V_{sc}/ \Delta I_L)\ D\ .\ T = 9.87$ mH

From the above, a standard value of 10 mH was chosen.

3.3.2 SIZING OF THE SUPERCAPACITOR

In general, the energy in the Supercapacitor is given by

$$E_{sc}=1/2\ .\ C_{sc}\ .\ V_{sc}^2 \qquad (41)$$

where E_{sc} is energy, C_{sc} is capacitance and V_{sc} is voltage of the SC. Defining lower limit of voltage (V_{scmin}) and relating $E_{sc}= P_{sc}\ t_d$ and solving for C_{sc} gives

$$C_{sc} =2\ P_{sc}\ t_d / (V_{scnom}-V_{scmin})^2 \qquad (42)$$

where t_d is the period of time that we want to eliminate fluctuation in WECS output, 120 seconds in this case. C_{sc} is the required capacitance to perform this function.

Now as P_{sc}= 0.75 MW, V_{scnom} = 1200 V, V_{scmin} = 100 V, t_d = 120 seconds then C_{sc} required is calculated to be 148.7 F using (42). This SC with a capacitance of C_{sc} has enough capacity to either extract or supply 0.75 MW of power for 120 seconds. The Buck-Boost converter was simulated with the following data to verify design:

P_{sc} =0.75 MW, C_{sc}=150 F, L=10 mH, V_{dclink}=1200 volts, f = 1620 Hz

Results are shown in Figure 10 & 11 for D=0.25 and D=0.75 respectively. Considering the Figure 10, the following data is observed (D=0.25):

Switching Frequency f = 1620 Hz.

Average I_L = 156 A

The value of $\Delta I_{L\text{-}on}$ = 25A

The value of t_{on} = 154.32 μs

The time period (T) = 617 μs

The V_{sc} = 300 V

The $V_{DC\text{-}link}$ = 1200 V

The power output of the SuperCapacitor = 0.0468 MW.

It is clear from the Figures 10 & 11 that magnitude of both current and voltage change as duty cycle D is varied. This change in voltage and current cause power to change and thus power can be adjusted by controlling D.

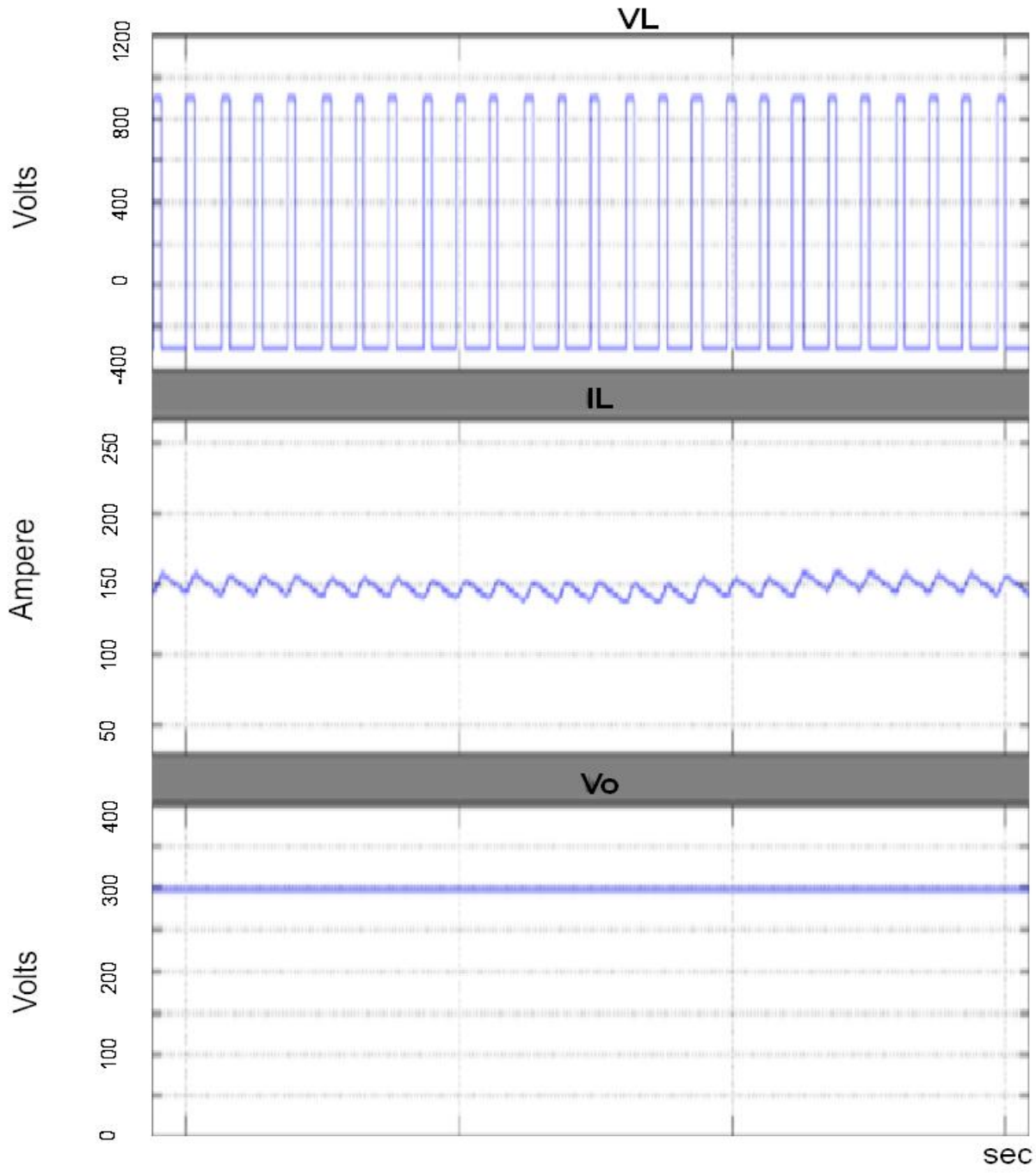

Figure 10: Simulation results with D=0.25

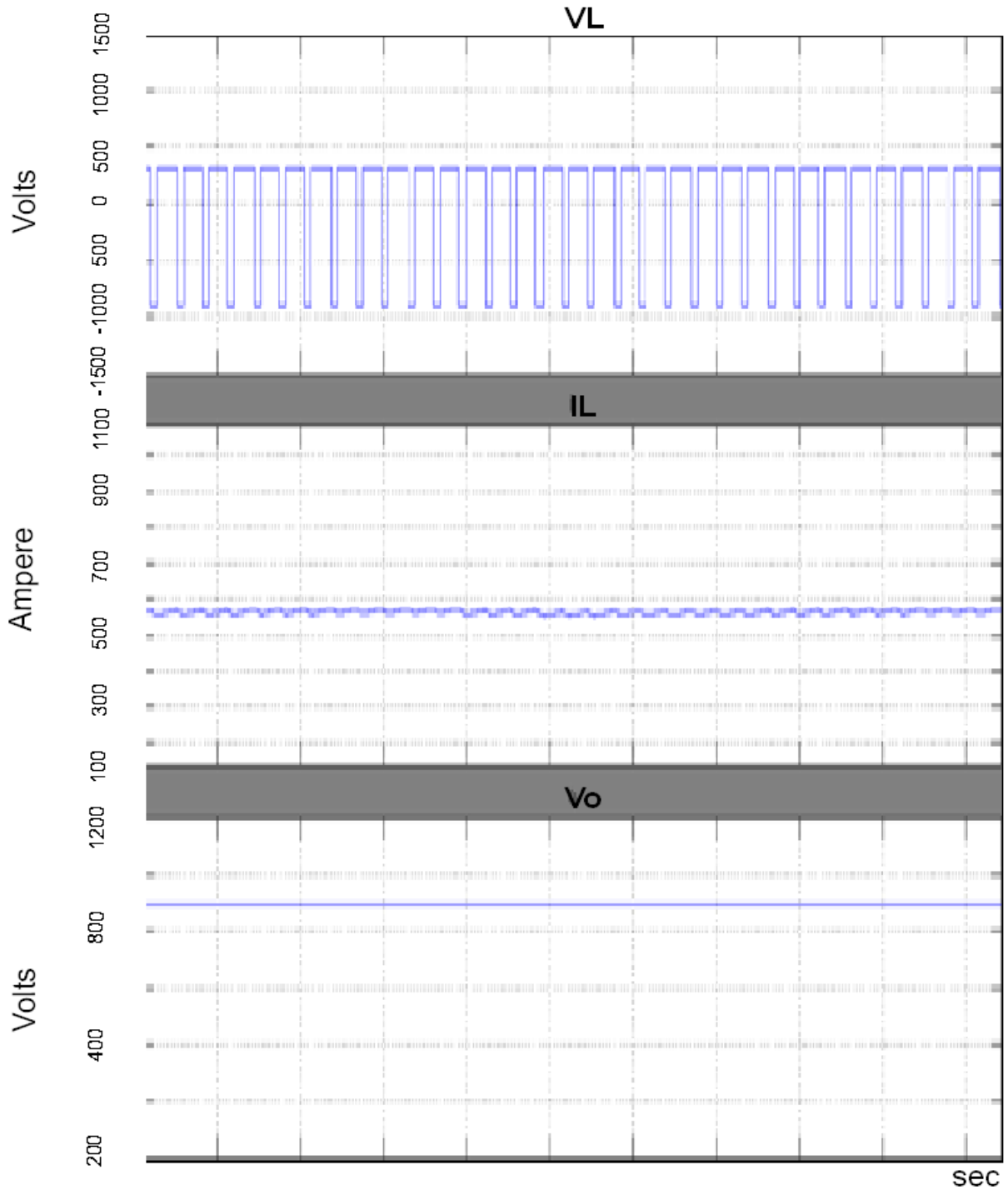

Figure 11: Simulation results with D=0.75

3.4 CONTROL SCHEME

Control scheme for the proposed topology shown in Figure 6 consists of System Limits Indicator (SLI), P_{ref} Setting System (PSS), Power Control System (PCS) and Operation Control System (OCS) as shown in Figure 12.

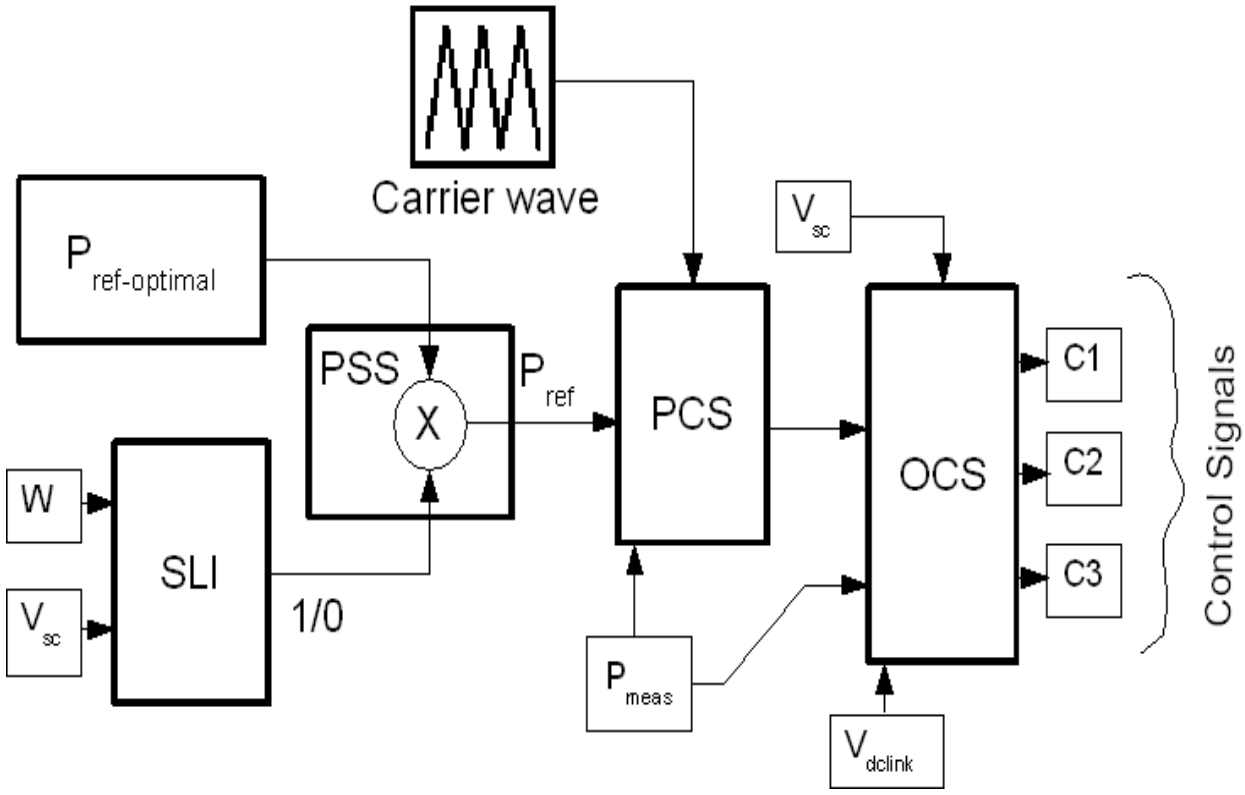

Figure 12: Control Scheme (proposed)

The following text explains the operating principle of the control scheme:

- SLI monitors wind speed (W) and voltage across SC (V_{sc}).
- SLI outputs a logic 1 if both $V_{sc}>V_{scmin}$ and $W>Wind_{cut\text{-}in}$ and its output equals 0 otherwise.
- PSS sets $P_{ref} = P_{ref\text{-}optimal}$ if SLI output is 1 otherwise P_{ref} is set to 0.
- PCS generates gating signals for the switching devices of the buck-boost chopper to maintain output of the DFIG (PO_t) equal to $P_{ref\text{-}optimal}$
- OCS
  - Keeps V_{dclink} and V_{sc} with in operating limits.
  - Passes gating signal from PCS.
  - Manages SESS

The system also displays different variables for monitoring including MPPT based instantaneous wind turbine power, PW_t. Now we will look at each of the building blocks of the control scheme one by one in detail.

3.4.1 SYSTEM LIMITS INDICATOR (SLI)

SLI shown in Figure 13 indicates whether system is operating in the defined working limits by measuring both V_{sc} and W. SLI checks for both V_{sc} and W and compares with their respective limits, V_{scmin} and $Wind_{cut\text{-}in}$ (DFIG-WECS turns on only if Wind speed > $Wind_{cut\text{-}in}$ otherwise it is turned off). SLI outputs logic zero if any limit is violated otherwise its output equals a logic one. Output of SLI is sent to PSS for further processing.

In this specific example, if V_{sc} is greater than 100 volts (V_{scmin}) and wind speed (W) is greater than 5 m/sec ($Wind_{cut\text{-}in}$), then the system is deemed to operate in the normal limits and this block outputs a logic value of 1 and otherwise outputs a value of 0. Referring to Figure 13, these comparisons are completed by two comparators. Outputs of the two comparators are logically intersected (AND) and sent to PSS for further processing.

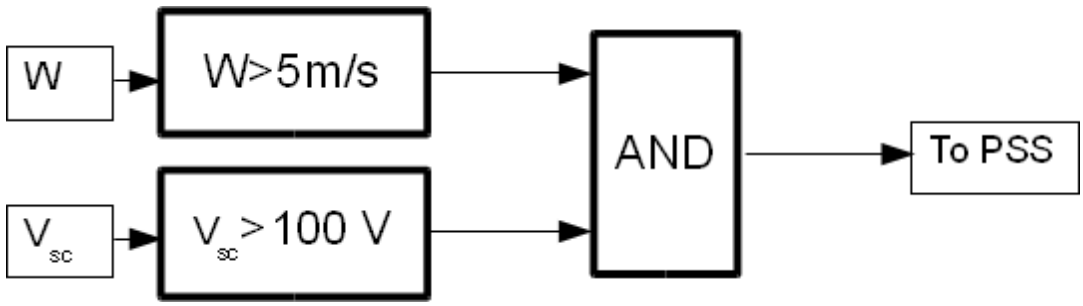

Figure 13: System Limits Indicator (proposed)

3.4.2 P_{ref} SETTING SYSTEM (PSS)

SLI output is received and used by PSS to set P_{ref} as shown in Figure 14. PSS sets $P_{ref} = P_{ref\text{-}optimal}$ ($P_{ref\text{-}optimal}$ is defined by POA and discussed in Chapter 5) if SLI outputs a logic one and sets power reference $P_{ref} = 0$ if SLI outputs a logic zero. Output of PSS is sent to PCS to generate gating signals. PSS also displays power reference set.

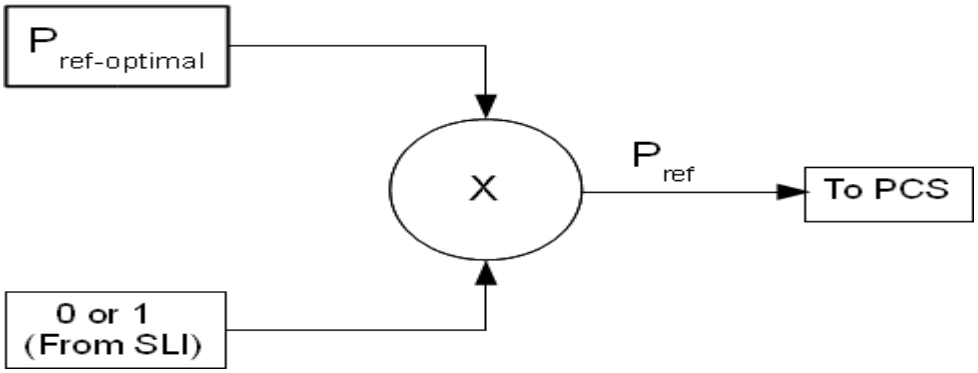

Figure 14: P_{ref} Setting System (proposed)

3.4.3 POWER CONTROL SYSTEM (PCS)

PCS generates gating signals for the chopper such that the DFIG's output power (PO_t) equals $P_{ref\text{-}optimal}$. As shown in Figure 15 carrier based PWM control system compares instantaneous output power measured (P_{meas}) with P_{ref} and passes difference through a Proportional-Integral (PI) controller for comparison with triangular carrier wave to generate a control signal. Depending upon whether this difference between P_{meas} and P_{ref} is greater or smaller than triangular wave, a logic zero or one is produced respectively, to turn DC-DC converter OFF or ON and thus keep output power in the vicinity of P_{ref}. This Control signal in essence controls operation of the DC-DC converter: a) to operate in the Buck mode when energy is transferred from DC-link capacitor to SC-Bank, and, b) in the Boost mode to transfer energy from SC-Bank to the DC-link capacitor. A train of pulses (zeros and ones) produced this way controls output power of the DFIG (PO_t) by either injecting into or extracting power from the Supercapacitor capacitor. This control signal is supplied to Operation Control System (OCS) for the final phase of the process.

P and I values used for PI controller are 0.7 and 10 respectively and were determined through a trial and error process.

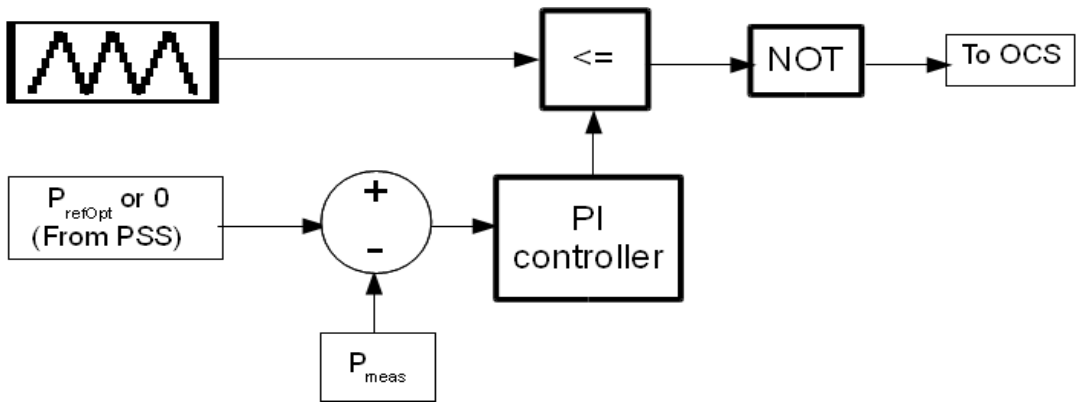

Figure 15: Power Control System (proposed)

3.4.4 OPERATION CONTROL SYSTEM (OCS)

The internal structure of OCS is shown in Figure 16. It outputs the gating signal (C1) to control chopper's operation, the Supercapacitor control signal (C2) to turn SC-Bank on or off and the System control signal (C3) to isolate the proposed SESS topology in the event of a failure. The following text explains the operation of OCS.

OCS receives the voltage signal V_{dclink} from the DC-link capacitor, the voltage signal V_{sc} from the Supercapacitor and the chopper gating signal from PCS. The magnitude of V_{sc} is limited between upper and lower limits of 1350 volts and 100 volts respectively. In a similar manner, the DC-link voltage is to be kept between 1000 volts and 1350 volts. If both of these variables (V_{sc}

and V_{dclink}) are within the limits then OCS produces the control signal C2 (binary) that either turns SC on or turns it off. If these same variables (V_{sc} and V_{dclink}) remain within their respective limits, then the gating signal from PCS is sent to the DC-DC converter as C1.

The measured output power of the DFIG WECS (P_{meas}) is used to determine whether SESS should be kept connected or not and accordingly produces a binary variable (C3). The comparator checks to see if P_{meas} is above zero. If this condition is not true, i.e. if P_{meas} equals zero, the SESS is isolated from the DFIG-WECS by setting C3 to 0.

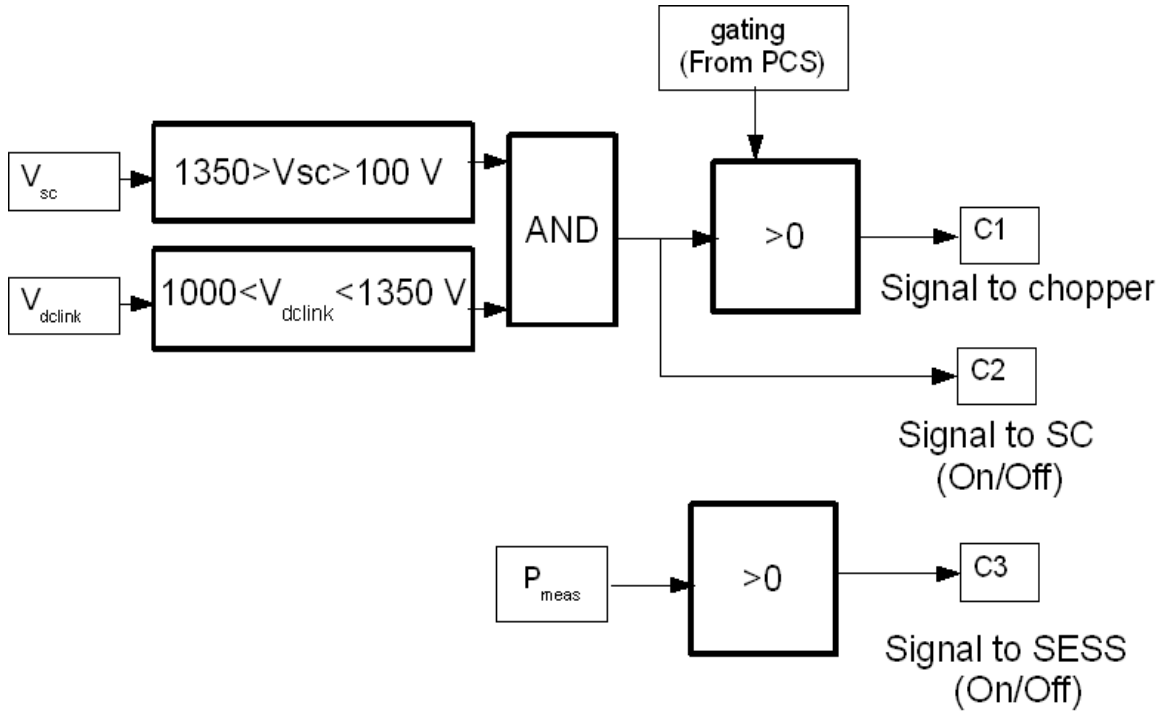

Figure 16: Operation Control System (proposed)

3.5 OPERATING PRINCIPLE

Referring to Figure 6 and discussion throughout this chapter the overall operating principle is as follows:

- $P_{ref\text{-}optimal}$ for given wind data is found by the Power Optimization Algorithm in Chapter 5.
- Control scheme blocks
    - The objective is to measure and control DFIG output to $P_{ref\text{-}optimal}$.
    - The SLI block determines if W and V_{sc} are within their limits.
    - PSS sets P_{ref} to equal $P_{ref\text{-}optimal}$ if SLI indicates normal operation.
    - PCS produces gating signal for the chopper to control output power (P_{meas}) of DFIG such that it equals $P_{ref\text{-}optimal}$.
    - OCS checks if all the voltages within the system are within their limits. If they are within their limits, it passes the gating signal to the chopper and enables the SC. It checks to see if output power is more than zero in which case it enables SESS operation.
- The DC-DC converter is controlled by OCS, in normal condition, to either work in Buck or Boost mode to extract or inject power to regulate output power P_{meas} such that it equals $P_{ref\text{-}optimal}$.
- SC-Bank works as either a storage or source of energy, as a storage in Buck mode to extract energy from DC-link capacitor and as a source in Boost mode to inject energy into the DC-link capacitor.

3.6 CONCLUSIONS

In conclusion, this chapter presents a topology to connect SC to the DFIG WECS through a chopper. The control system for the chopper is presented. The design for the chopper and control system are presented as well.

In the next Chapter, an example of the working of the proposed topology and the inner control loop are presented.

CHAPTER 4

SIMULATION RESULTS

4.1 INTRODUCTION

In this chapter of the thesis, we look at the response of DFIG-WECS with the proposed SESS topology and the inner control loop. This response is compared with the performance of DFIG-WECS without the proposed SESS topology. Various system parameters are measured in both cases and compared to arrive at conclusions. In order to facilitate this comparative study, we select a data set for wind pattern having 120 points. The wind pattern is shown in Figure 17.

4.2 DFIG-WECS OPERATION WITHOUT PROPOSED TOPOLOGY

In this section of the chapter, we look at the response of DFIG-WECS without the proposed SESS topology. Simulation results are shown in Figures 18-22 for the wind pattern shown in Figure 17 that lasts for 120 seconds. The net energy in wind for 120 seconds equals 48.1 MW-s and the average power is equal to 0.401 MW.

It may be observed in Figure 20 that the DC link voltage remains at 1200 V and that output reactive power in Figure 19 remains at 0 Mvar despite a changing output real power. These are achieved by the control system of the Grid Side Converter that works independent of the proposed SESS system.

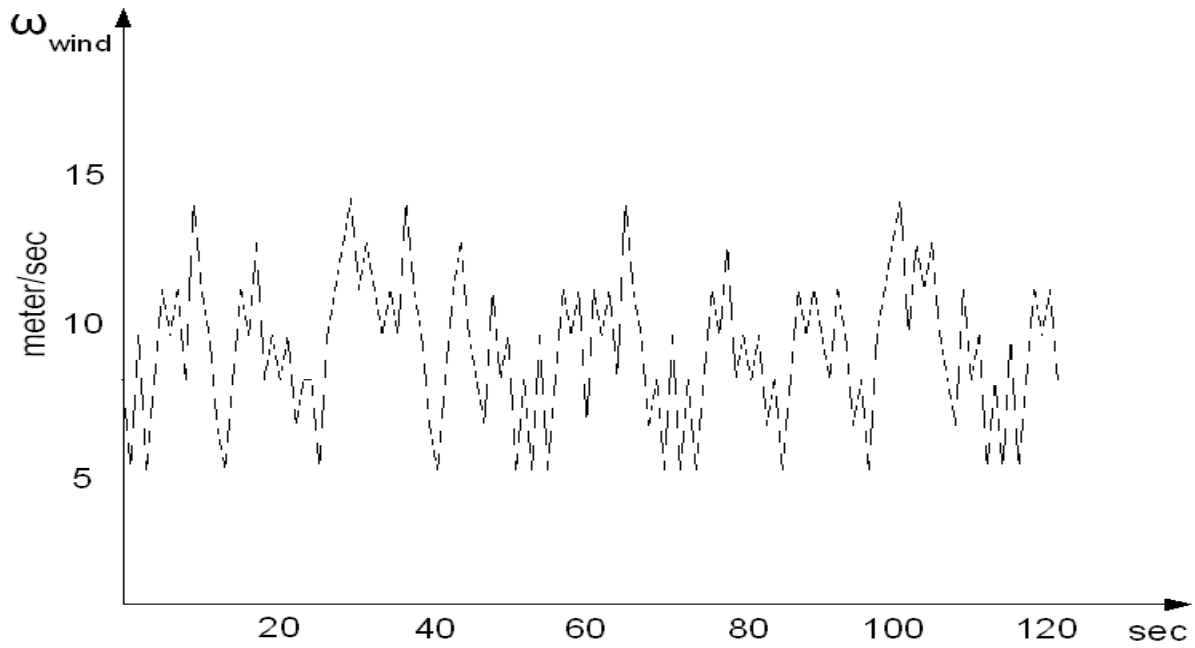

Figure 17: Wind pattern (120 Sec)

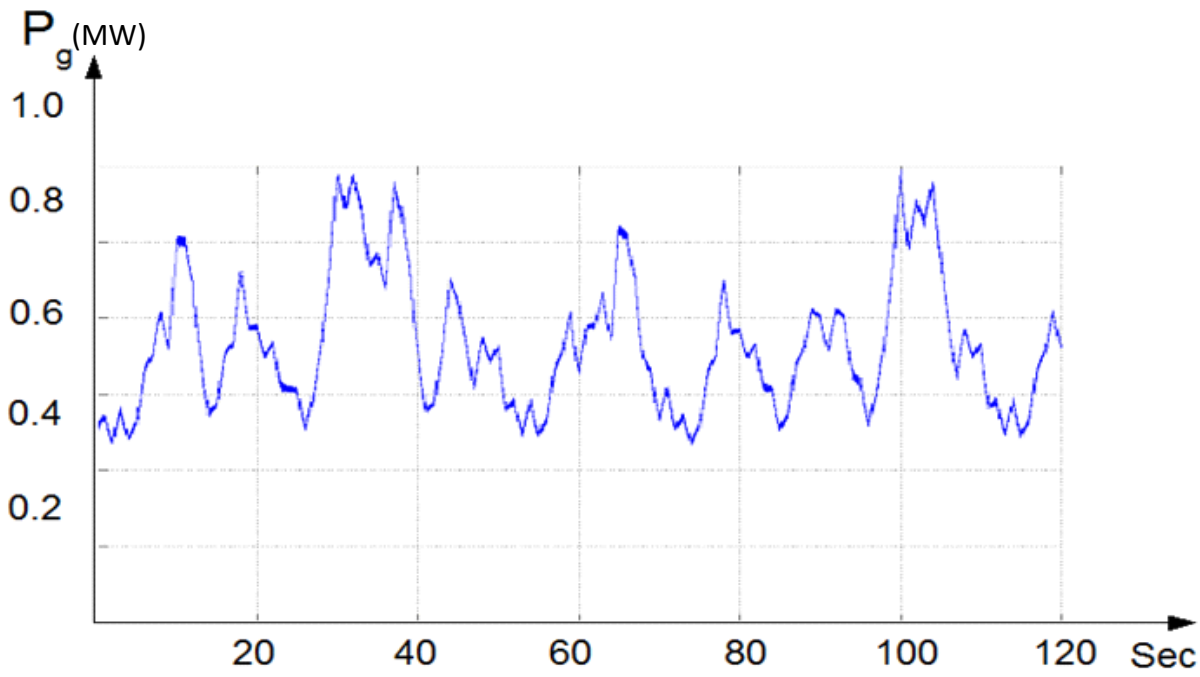

Figure 18: Grid Active power

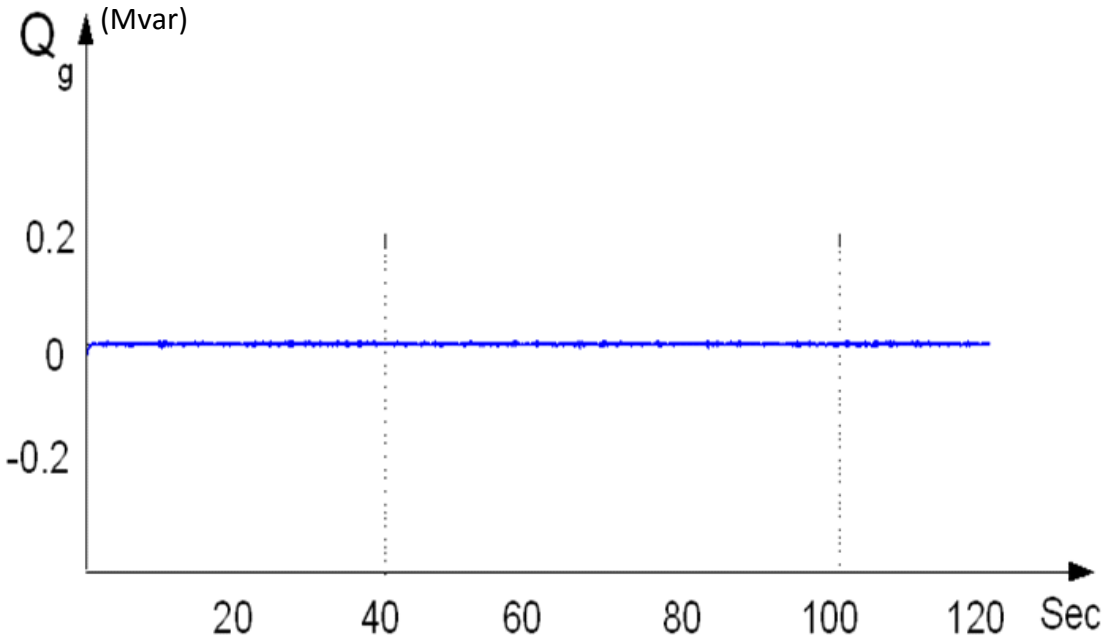

Figure 19: Grid Reactive power

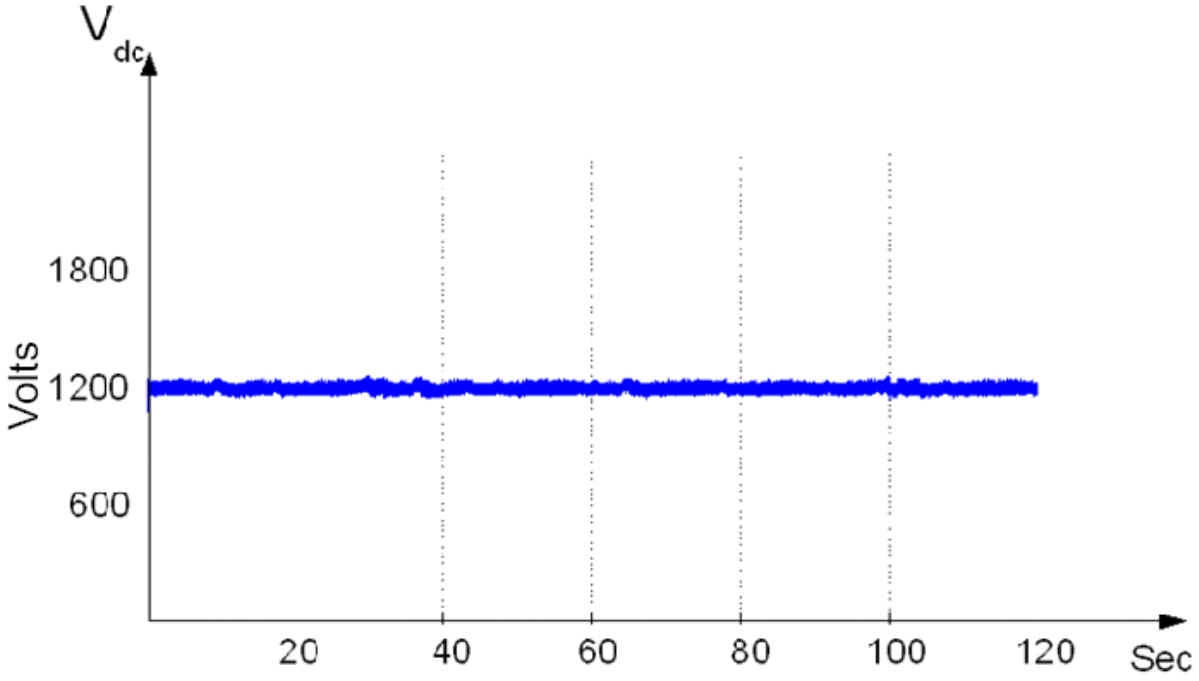

Figure 20: DC-link voltage (V)

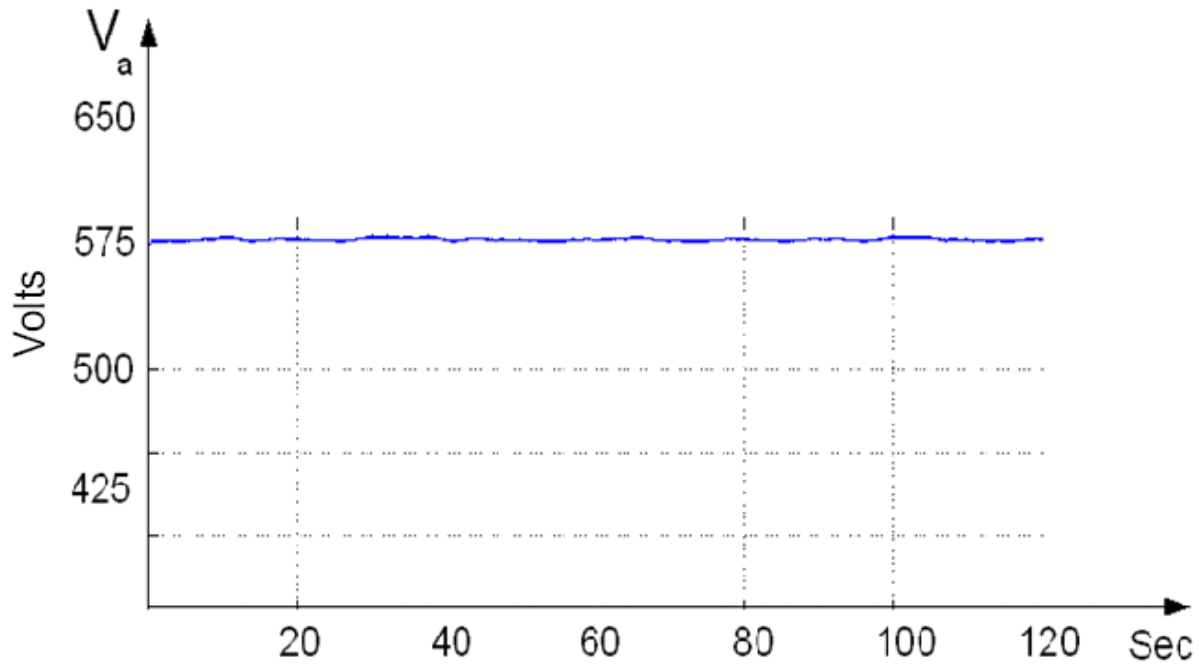

Figure 21: Grid voltage (V)

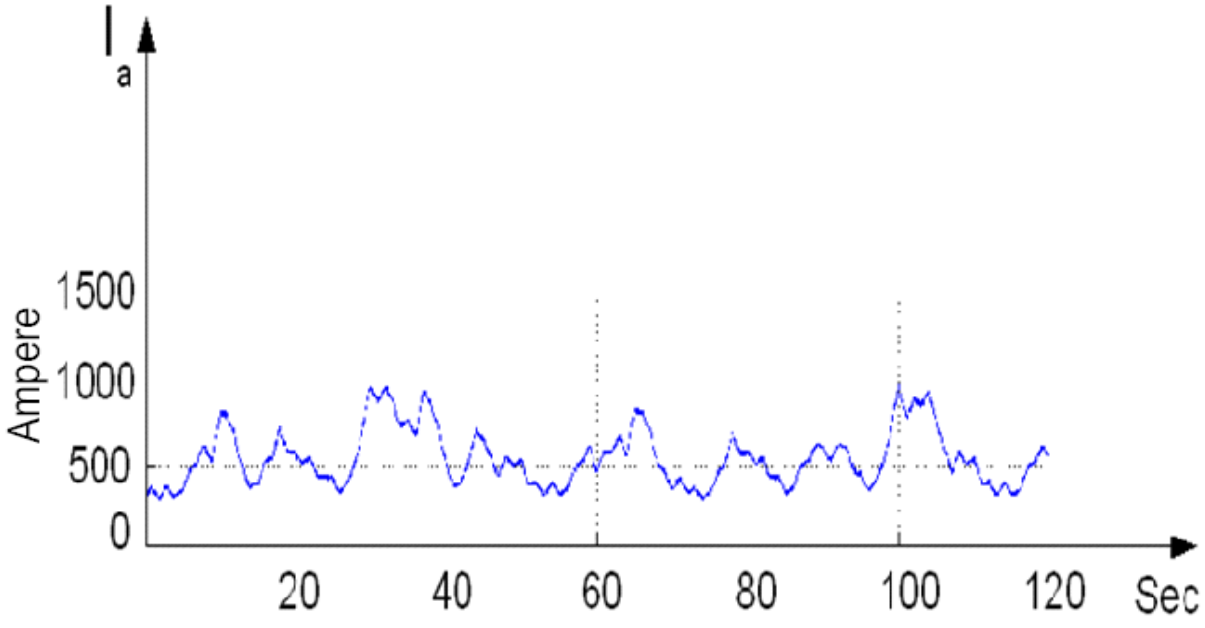

Figure 22: Phase a Current (A)

From the Figure 18, one can see that all of the input power from the wind turbine reaches to the output of the DFIG. This output power is highly variable.

4.3 DFIG-WECS OPERATION WITH PROPOSED TOPOLOGY

This section discusses response of DFIG WECS with the proposed SESS topology and the inner control loop. The results are shown in Figures 23-28 for the same wind pattern shown in Figure 17. It is a two-step procedure:

- The optimal output power reference level for DFIG-WECS is established for the given wind pattern using the optimization technique proposed in Chapter 5. This value is $P_{ref\text{-}optimal}$ and it equals 0.401 MW in this example.
- The WECS output power (power injected into the grid by WECS) is controlled around this optimal power reference level, $P_{ref\text{-}optimal}$ by SESS and the inner control loop.

Analyzing graphs in Figures 18 and 23 and comparing them, the following is seen. The power output of DFIG-WECS <u>without</u> SESS system is variable and follows the wind power. However, it can be seen that the output of DFIG-WECS <u>with</u> the SESS system and inner control is nearly constant. This constant value equals the $P_{ref\text{-}optimal}$ value of 0.401 MW as determined by the optimization algorithm presented in Chapter 5.

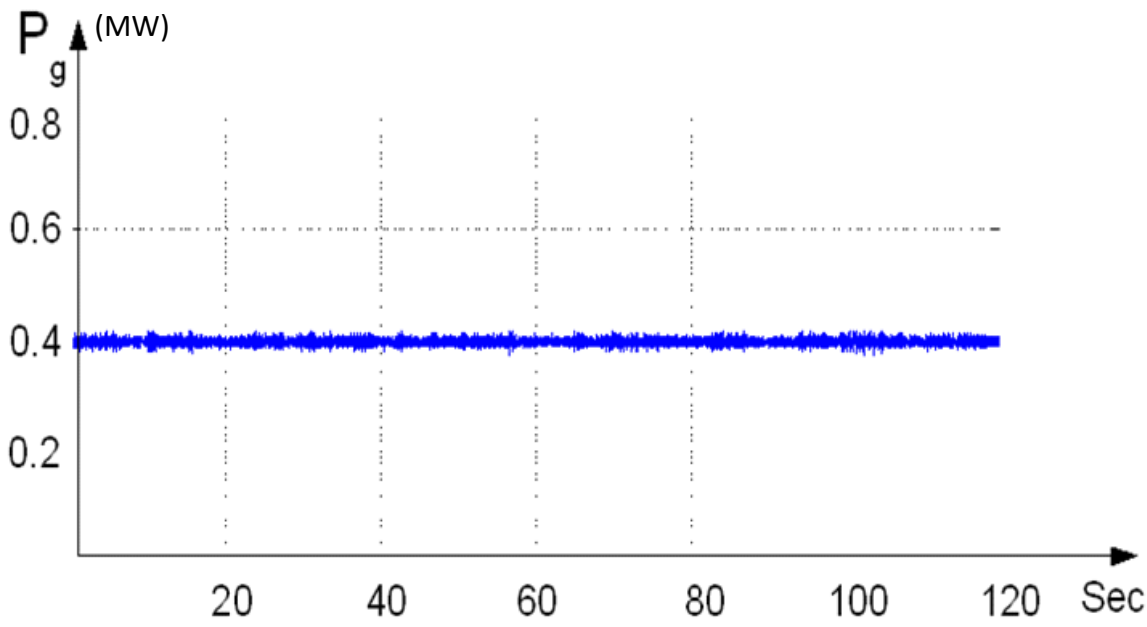

Figure 23: Grid Active power

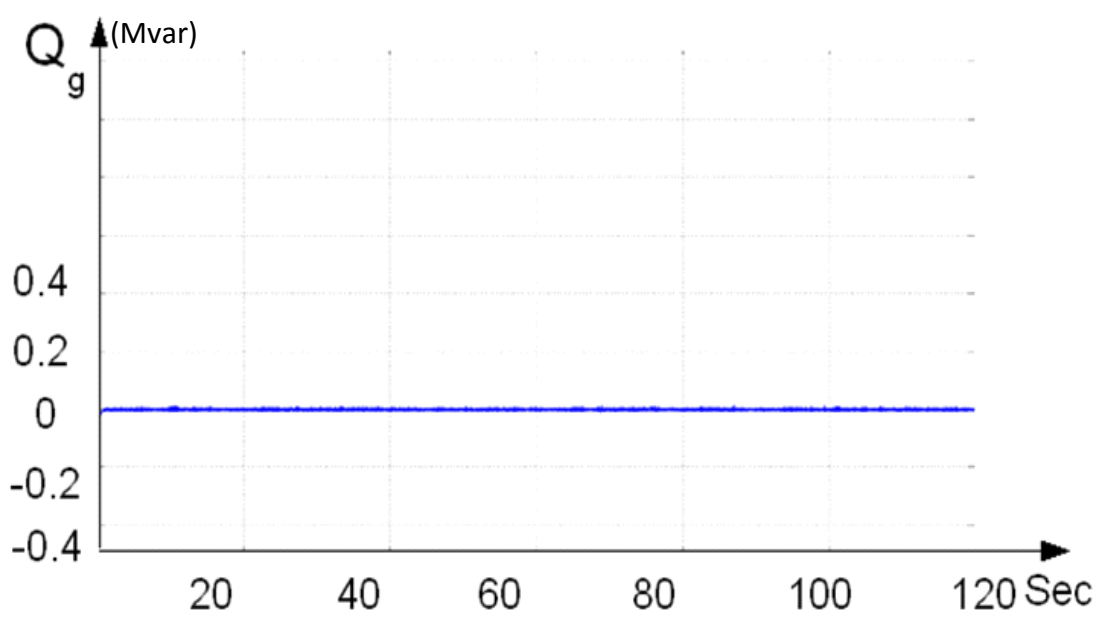

Figure 24: Grid Reactive power

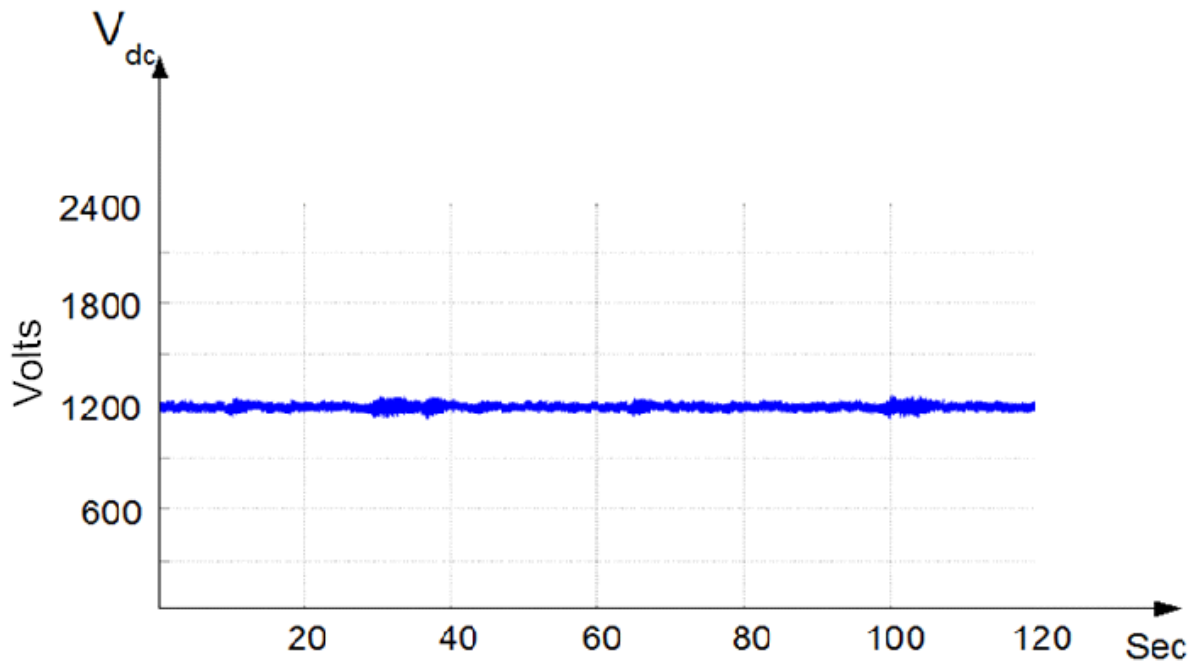

Figure 25: DC-link voltage (V)

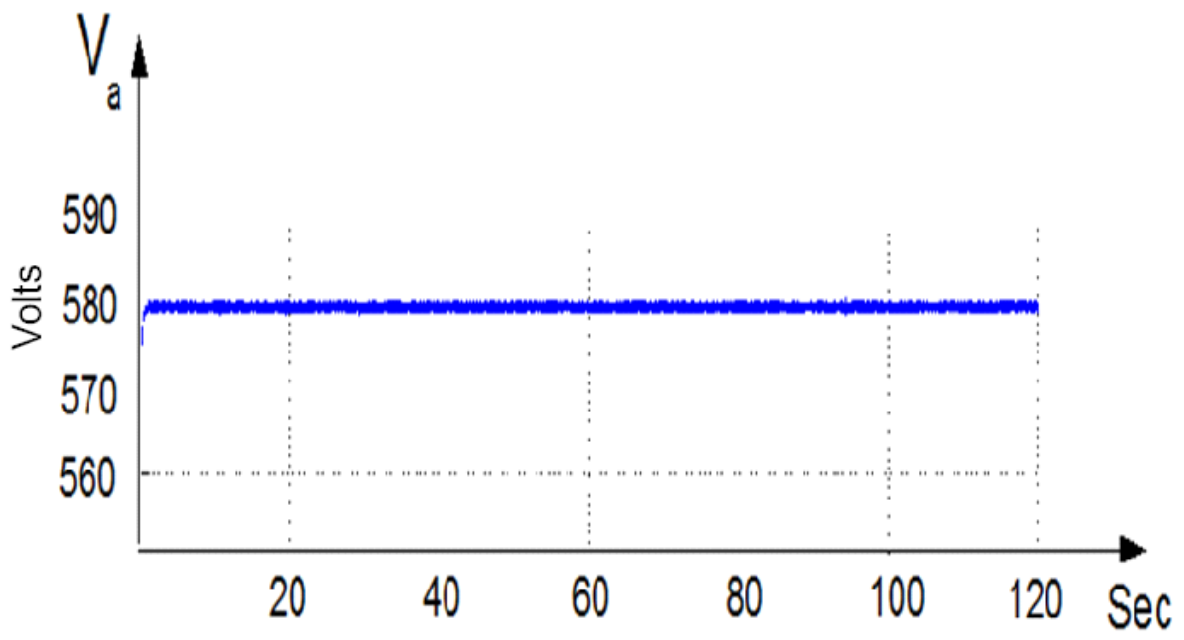

Figure 26: Grid Voltage (V)

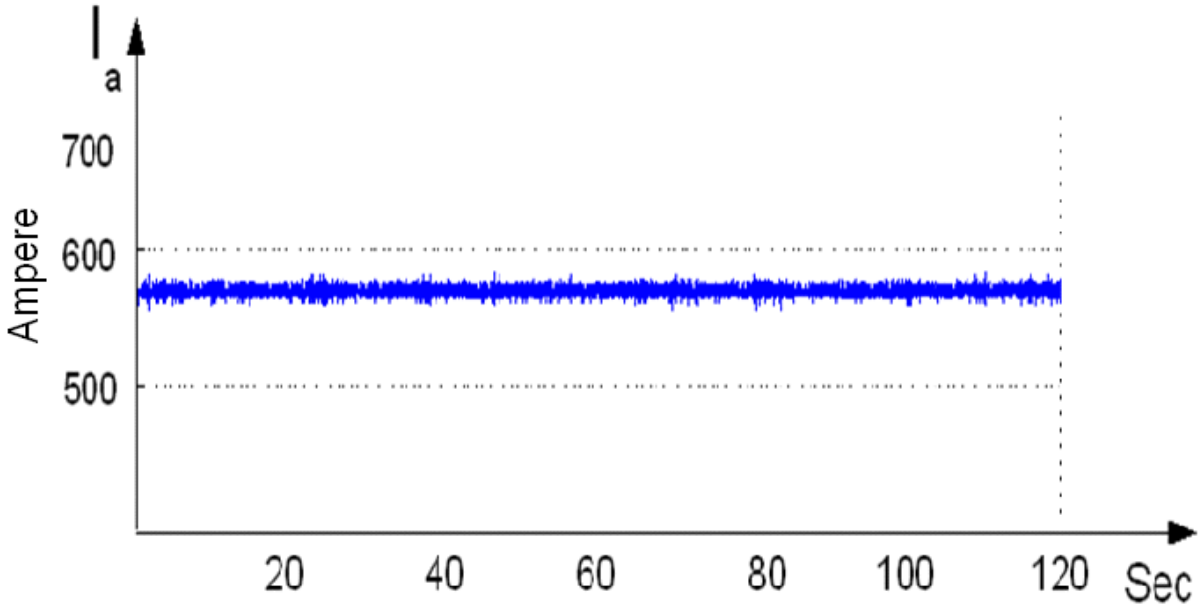

Figure 27: Phase a Current (A)

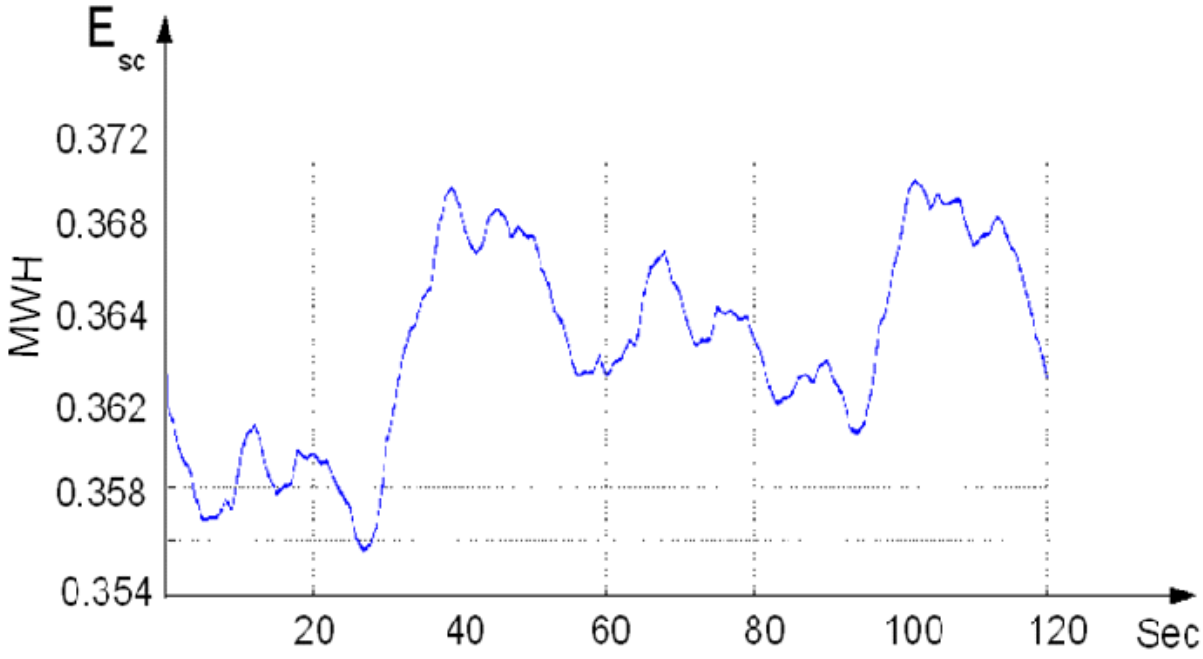

Figure 28: SC Energy (MWs)

4.4 CONCLUSIONS

Looking at the responses of the system in Figures 18-22 in section 4.2 (DFIG-WECS without proposed topology) and Figures 23-28 in section 4.3 (DFIG-WECS with proposed topology) following can be observed:

- DC-link voltage is almost same in both cases, around 1200 volts.
- Grid voltage is almost same in both cases, 575 volts.
- Reactive power is same in both cases, maintained at zero.
- Phase current varies from 320 A to 930 A without the proposed topology and is constant around 570 A with the proposed topology.
- Active power changes from 0.35 MW to 0.90 MW without proposed topology and is maintained around an average power of 0.401 MW with proposed topology.
- SC energy starts from, and ends with, 0.363 MW-s of energy while it varies in the 120 seconds in between due to charging and discharging commands from the inner control loop.
- The total energy extracted from wind is supplied into the grid in both cases.

Thus, it is clear from the graphs and remarks above that the energy in the SC changes due to continuous charging and discharging. This is done to keep the output power of DFIG-WECS at a constant value. This charging and discharging of the SC is accomplished by controlling the duty cycle of the buck-boost converter. It is noticeable that the proposed optimization algorithm

ensures that the energy in the SC at the start and the end of the 120 seconds remains the same whereby the net energy from wind is transferred to the connected electric network. The total energy supplied into the grid (0.401 MW x 120 sec = 48.1 MW-s) equals energy extracted from wind (48.1 MW-s). Therefore, it is concluded that the integration of the proposed SESS topology and the proposed optimization algorithm (chapter 5) with DFIG-WECS can improve quality of the power supplied into the grid despite of the fluctuating nature of the wind speed.

CHAPTER 5

POWER OPTIMIZATION ALGORITHM

5.1 INTRODUCTION

The nature of wind speed is intermittent and thus power produced by WECS is intermittent as well. In order to avoid injecting this irregular power into the grid, a mechanism to smoothen this intermittence is required. The goal here is to keep power produced by WECS at a constant value or a minimum set of constant values subject to operating limits. Such a solution must ensure that the total extractable wind energy is delivered into the connected power grid. Referring to Figure 6 and discussions in Chapter 3, the chopper's control system receives a $P_{ref\text{-}optimal}$ value. The inner control loop proposed in Chapter 3 along with the SESS holds the DFIG's output to this value eliminating short-term power fluctuations and supplies a constant power into the grid. This chapter presents an optimization algorithm that determines this $P_{ref\text{-}optimal}$ for a given wind speed data and forms the outer control loop.

5.2 PROBLEM FORMULATION

Consider that the optimization is completed for NH periods with each period representing a duration of NX seconds. The total power input into and output from the supercapacitor is limited

by the capability of itself and the connected chopper. Considering all the constraining elements, the maximum input in the tth instant ($PC_t < 0$) when the supercapacitor is charging is given by PC_{min}. Similarly the maximum output capacity of the supercapacitor is given by PC_{max}. Constraining the tth instant power input/output of the supercapacitor to these limits, the following constraint may be formulated:

$$PC_{min} < PC_t < PC_{max} \quad ; \forall\ t = 1 \text{ to } NH \tag{43}$$

The net output in the tth instant (PO_t) of the DFIG is constrained by the max equipment rating of PO_{max}. Accordingly, the tth instant power output is constrained as below:

$$0 < PO_t < PO_{max} \quad ; \forall\ t = 1 \text{ to } NH \tag{44}$$

The variable PC_t is the power input/output of the supercapacitor in the tth instant. Multiplying it by NX seconds (numerically equal to NX. PC_t) represents the energy input/output of the supercapacitor. Since we do wish to store or take any energy at the end of the NH periods and ensure that energy in the supercapacitor remains unchanged, the following constraint is enforced.

$$\Sigma_t\ PC_t = 0 \tag{45}$$

The min and max amount of energy that can be stored in the supercapacitor at any instance is given by EC_{min} and EC_{max}. In the tth instant, adding energy input/output from preceding instants ($\Sigma_{k=1:t}$ NX. PC_k) to the initial energy EC_0, one may determine the total energy. This total energy in the tth instant is constrained to be within the supercapacitor energy capacity as below:

$$EC_{min} \leq EC_t = EC_0 + \Sigma_{k=1:t}\ NX\ .\ PC_k < EC_{max} \quad ; \quad \forall\ t = 1 \text{ to } NH \tag{46}$$

In the tth instant, the system power balance is described by the equality below that ensures that

the power from the wind turbine is either channelled to the SC or output of DFIG:

$PW_t = PC_t + PO_t$; $\forall$ t = 1 to NH (47)

If in the tth instant, the output increases by any value, then the variable US_t assumes a value of 1 and remains at zero otherwise. Similarly, if in the tth instant, the output decreases by any value, then the variable UD_t assumes a value of 1 and remains at zero otherwise. In each instant their values remain between 0 and 1 and hence they can be constrained as a below. It must be borne in mind that these are integer variables.

$0 < US_t < 1$; $\forall$ t = 1 to NH (48)

$0 < UD_t < 1$; $\forall$ t = 1 to NH (49)

The change in power of the whole DFIG from the tth instant (PO_t) and the next instant (PO_{t+1}) is given by (PO_{t+1} - PO_t). The integers UD_t and US_t track these changes if there is decrease or increase respectively and limit it to $\pm PO_{max}$. In the absence of a decrease or increase, this change (PO_{t+1} - PO_t) should be equal to zero. This is represented concisely as a below:

$-PO_{max} .D_{,t+1} < PO_{t+1} - PO_t < PO_{max} (US_{t+1})$; t = 1 to NH-1 (50)

Since the power can either increase or decrease in the tth instant:

$0 < US_t + UD_t < 1$; t = 1 to NH (51)

The objective of the optimization is to minimize the number of changes in the power output, thus:

Minimize: $\Sigma_t (US_t + UD_t)$ (52)

Subject to constraint (43)-(51).

This proposed formulation was solved to minimize the number of output power changes subject

to the limits and constraints defined above. Two solution techniques are proposed to solve the power output optimization challenge and they are:

- Iterative Search Technique (IST)
- Mixed Integer Linear Programming Technique (MILPT)

These algorithms are presented in the following text. These algorithms were tested on a wind speed data set with 12 points. The wind speed is in meters/sec and power in Megawatts.

Wind = [7 6 8 6 11 10 11 11 12 11 10 11] m/s

Power = [0.2 0.12 0.29 0.12 0.73 0.55 0.73 0.73 0.95 0.73 0.55 0.73] MW

Total Energy = 6.43MWs

5.3 ITERATIVE SEARCH TECHNIQUE (IST)

This method of output power optimization is based on an iterative search. The method searches for the minimum set of fixed output values ($P_{ref\text{-}optimal}$). Parameters such as wind data, SC initial energy and operating limits are considered in the optimization method. From the wind speed and power data, the average wind power value is determined. This average value is an initial guess for the constant output power of DFIG ($P_{ref\text{-}optimal}$) and the number of output levels is one (the minimum possible). The algorithm then checks to see if the initial guess satisfies operating constraints such as converter rating etc. If the constraints are satisfied, then the solution is retained as the optimal solution. If the constraints are not satisfied, then the algorithm repeats this set of steps with one more output level in an incremental manner until it finds the optimal solution.

5.3.1 IST Algorithm

Step 1: Variables (wind pattern, counters, etc) are declared and initialised

Step 2: Rated power, minimum and maximum limits and initial status of the devices are defined

Step 3: The total wind energy for given wind pattern is calculated

Step 4: $P_{ref\text{-}optimal}$ is found by simple averaging the data points

Step 5: An iterative search is initiated to determine $P_{ref\text{-}optimal}$ values such that the minimum set of output values are used.

Step 6: The optimal $P_{ref\text{-}optimal}$ value is recorded

5.3.2 IST Results

The data set presented in Section 5.1 is used for analysis. The results of scheduling are presented in Figures 29 and 30. By analyzing the graphs in Figures 29 and 30, one level of output power transfers the varying wind power. The difference between the output power and input wind power is stored or released appropriately from the supercapacitor. This ensures that the grid sees a static power output. Matlab code and simulation results for data sets with 120 samples and 600 samples with an initial energy that equals 50% of the supercapacitor's capacity are provided in Appendix A.

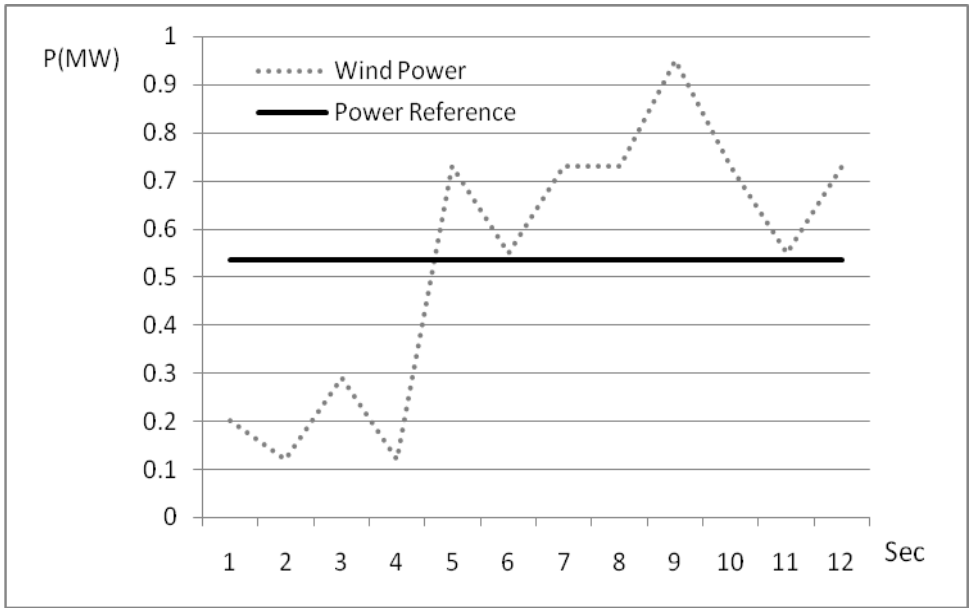

Figure 29: Wind power & power reference (IST)

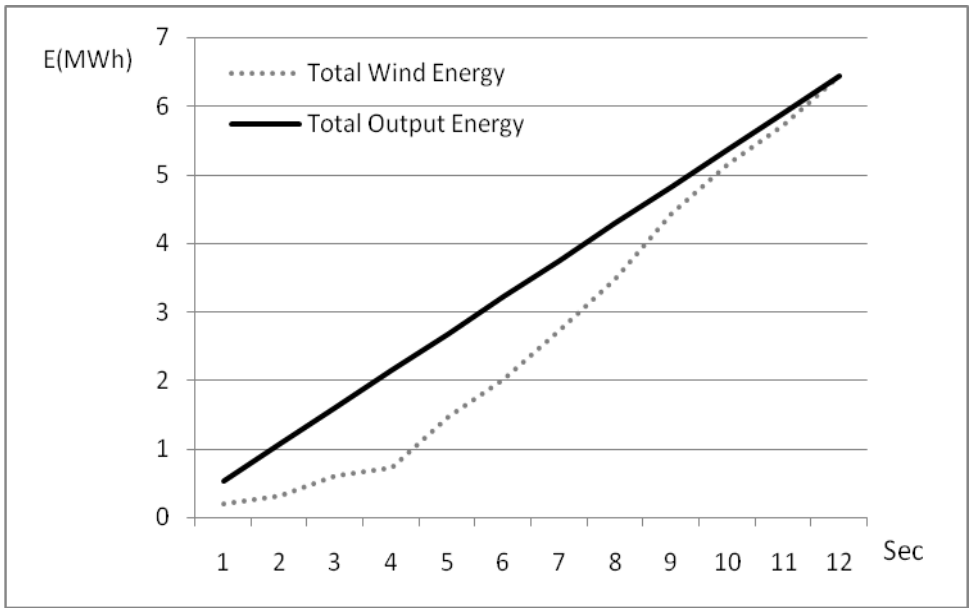

Figure 30: Total wind and IST Energy

5.4 MIXED INTEGER LINEAR PROGRAMMING TECHNIQUE (MILPT)

The goal here, as before, is to minimize the number of output power levels and thus minimize output power fluctuations. The proposed method solves the formulation in (52) with constraints in (43)-(51) using the MILP technique.

5.4.1 MILPT Algorithm

The formulation above (43)-(52) is programmed in MATLAB® and solved using the optimization function "mosekopt", an optimization toolbox. The proposed algorithm is given below:

Step 1: Variables are declared and initialised

Step 2: Constraints and limits are defined based on devices ratings, initial status and other operational constraints

Step 3: The formulation (43)-(52) is solved to minimise number of output power levels

Step 4: The $P_{ref\text{-}optimal}$ and other variables are recorded and plotted

5.4.2 MILPT Results

The data given in Section 5.1 is used for determining the optimal set of value for the DFIG. The output power and energy from DFIG are shown in Figures 31 and 32. It can be seen that a constant power output with one level is the optimal solution as shown in the previous algorithm as well. The power supplied to the grid is constant and free of fluctuations. The Matlab code and simulation results for data sets having 120 samples and 600 samples with an initial supercapacitor charge of 50% of full capacity are provided in Appendix B.

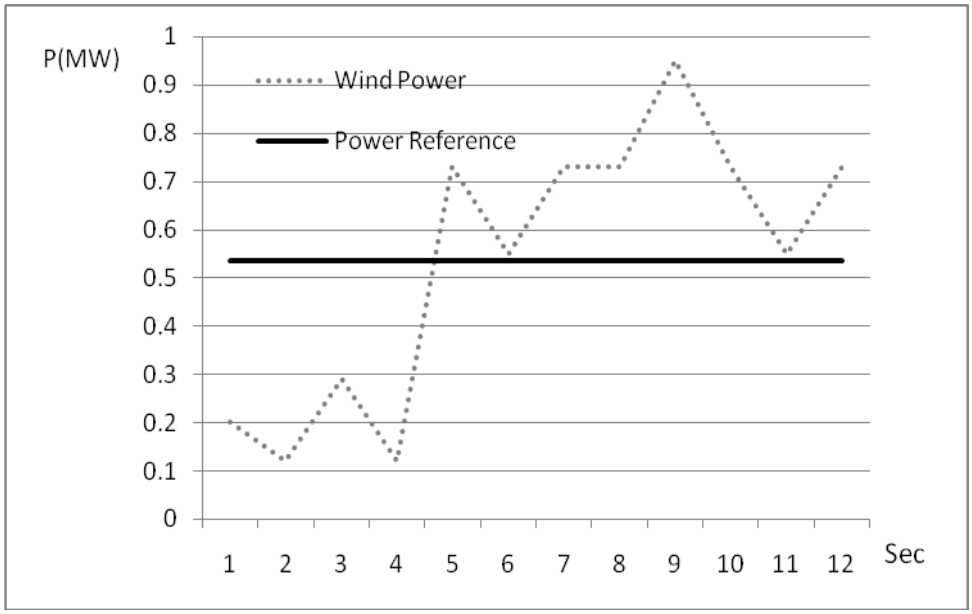

Figure 31: Wind power & power reference (MILPT)

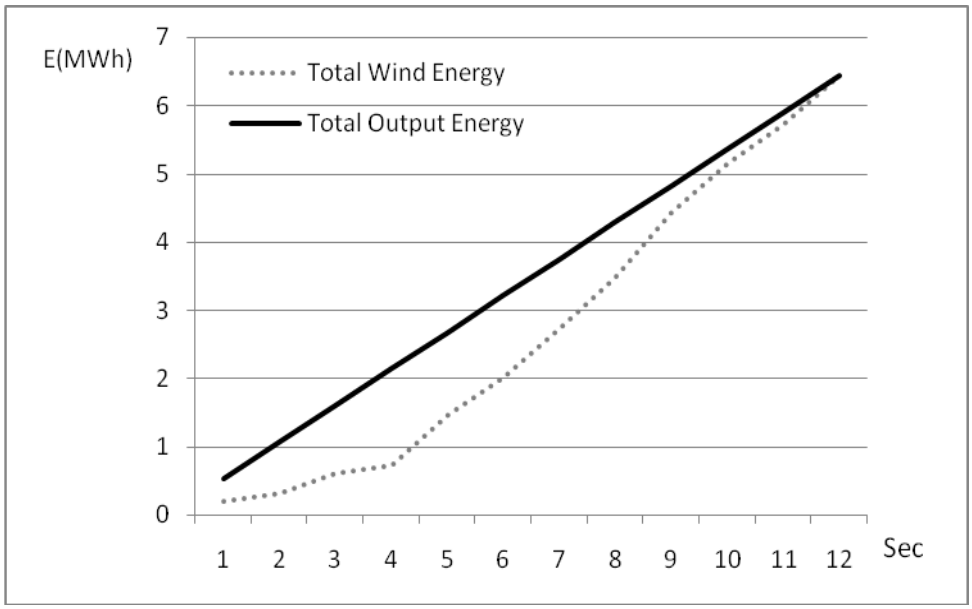

Figure 32: Total wind and MILPT Energy

5.5 EFFECT OF SC INITIAL ENERGY

The energy in the supercapacitor plays a vital role in stabilizing the output of the DFIG. This section considers a data set with 600 points of wind power for 600 seconds. This data is scheduled using the MILPT algorithm proposed in the previous section. The results of scheduling the system with three cases are presented Figure 33, 34, and 35. Figure 33 shows the optimal schedule of the system power output with an initial energy of the supercapacitor at the minimum value of zero. It delivers the output at three levels. Figure 34 shows the optimal output power of the system with the initial energy of the supercapacitor at its maximum. It shows the optimal schedule in this case with output power at three levels. Thereafter, Figure 35 shows the output power for case where the initial energy equaled 50% of the supercapacitor's capacity and in this case the number of output levels equal one. Hence, when the supercapacitor's charge is at 50% of its capacity, the output has the least number of power levels.

Thereafter, for various values of initial energy expressed in percentage of the total energy capacity of the supercapacitor, the minimum number of output power levels is determined and presented in Figure 36. Very clearly, it can be seen that with a half charged supercapacitor, the system has the minimum number of output levels.

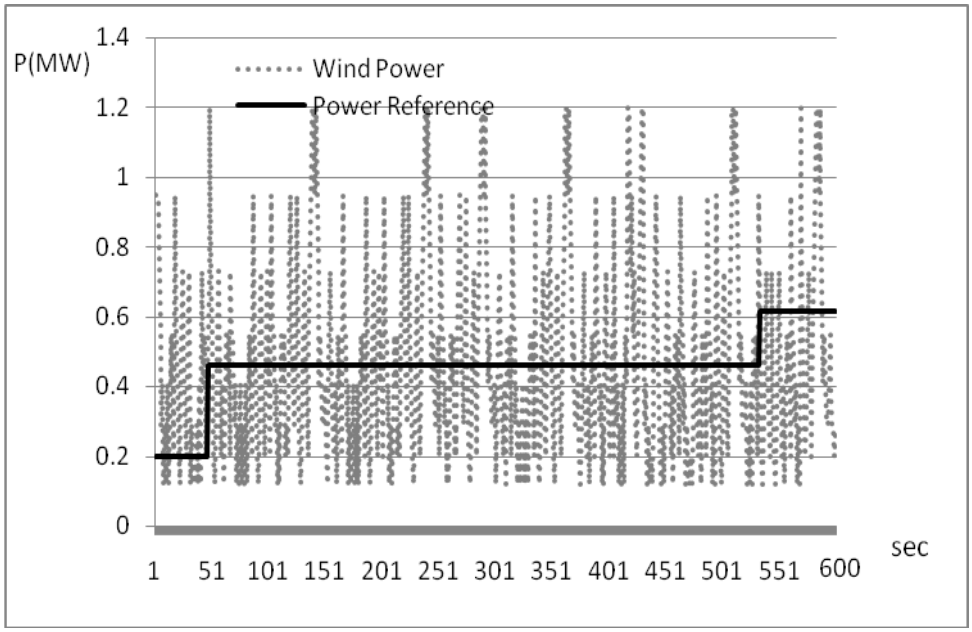

Figure 33: $P_{ref\text{-}optimal}$ with zero initial energy in the supercapacitor

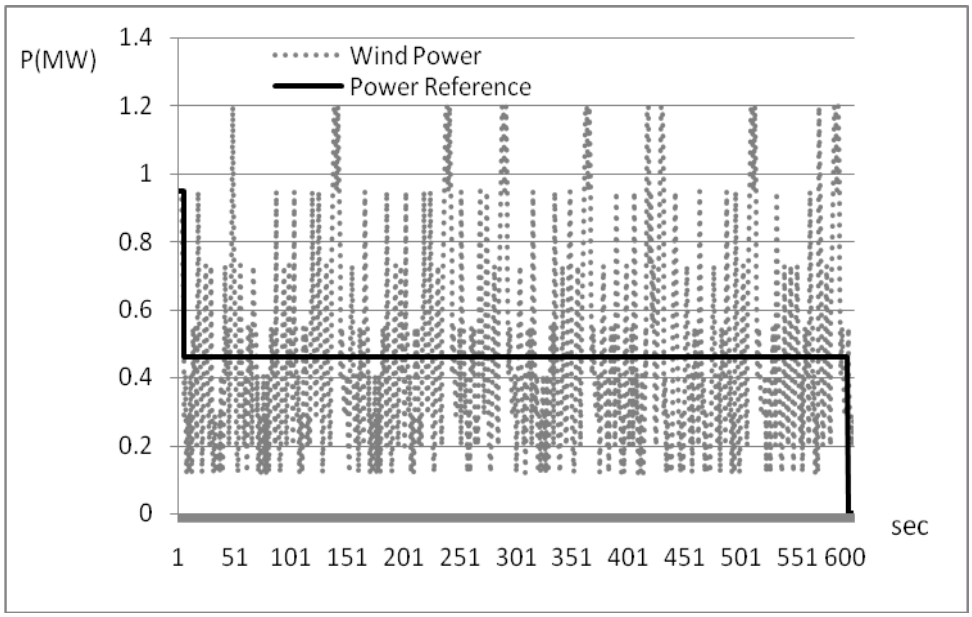

Figure 34: $P_{ref\text{-}optimal}$ with initial energy in the supercapacitor at its maximum

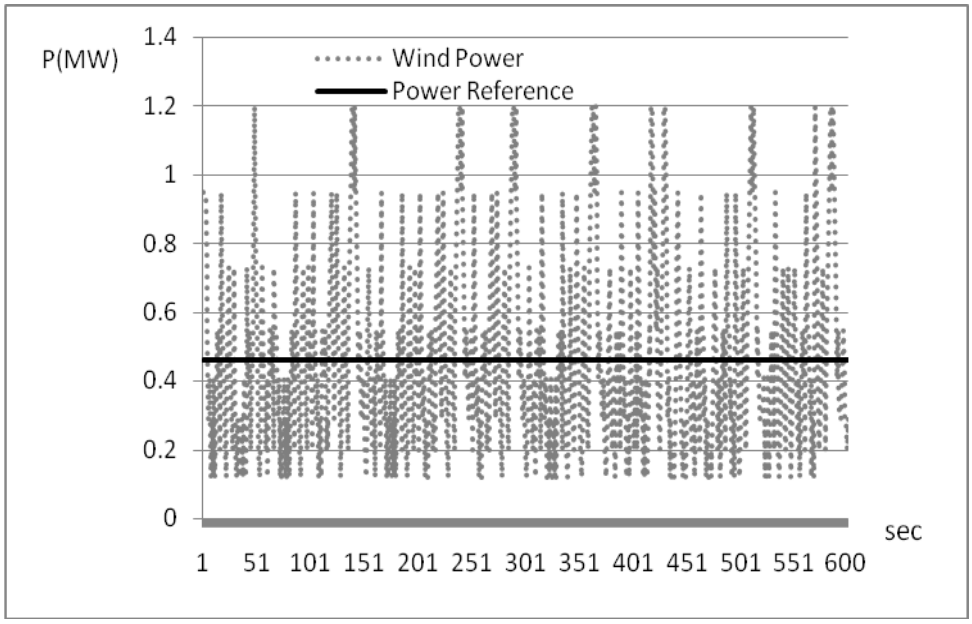

Figure 35: $P_{ref\text{-}optimal}$ with initial energy in the supercapacitor at 50% of its capacity

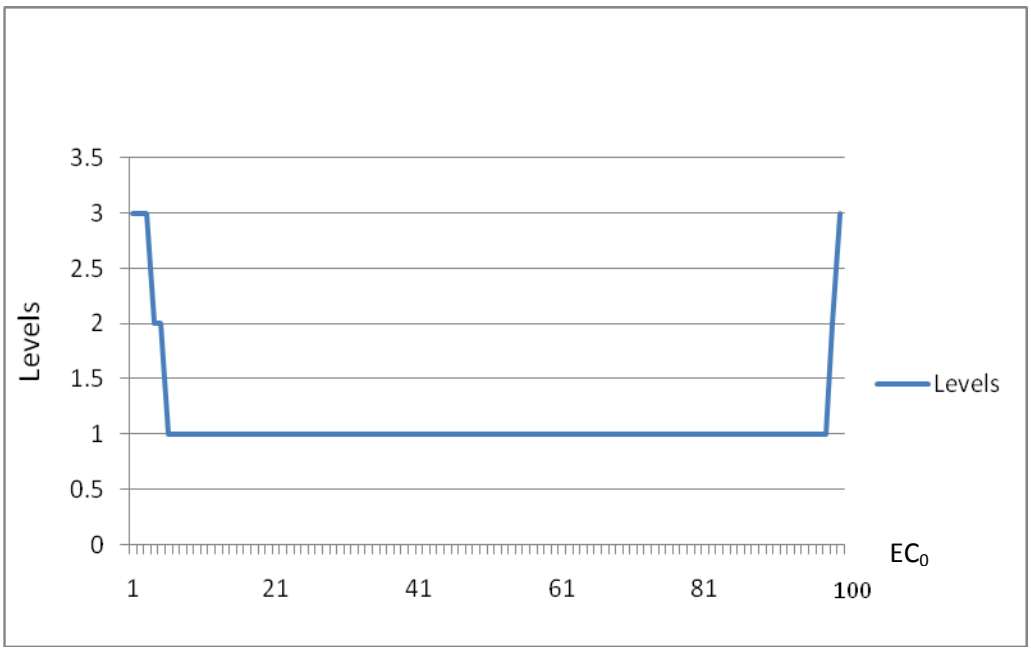

Figure 36: Effects of initial energy in the supercapacitor expressed as a percentage of its capacity

5.6 ALGORITHMS COMPARISON

Discussions and graphs above clearly show that both IST and MILPT are effective in eliminating fluctuations and thus improving power quality of the output of the DFIG. These techniques are compared in this section.

Two wind patterns with 120 data points each are considered for analysis. The effect of changing the SC's initial energy, expressed as a percentage of its total capacity, is shown in Figure 37 and 38 for pattern 1 and Figures 39 and 40 for pattern 2.

From the graphs, one may easily see that when the initial energy of the supercapacitor is close to 50%, the two methods perform well and have one output level.

When the SC has a very low or a very high initial energy that is closer to 0% or 100%, then there is more output levels. Then it those cases, MILPT get a lesser number of output levels.

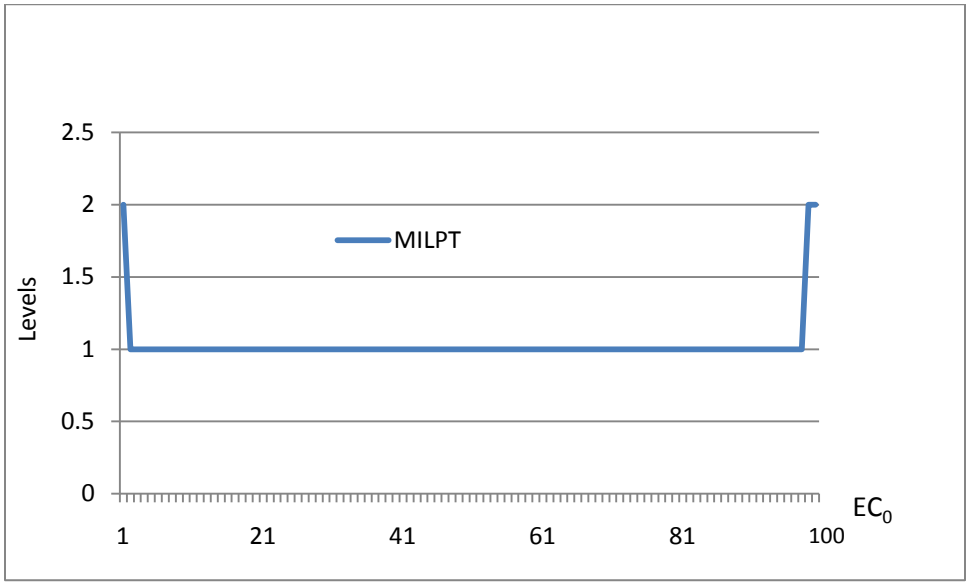

Figure 37: EC_o effect on MILPT Wind Pattern-1

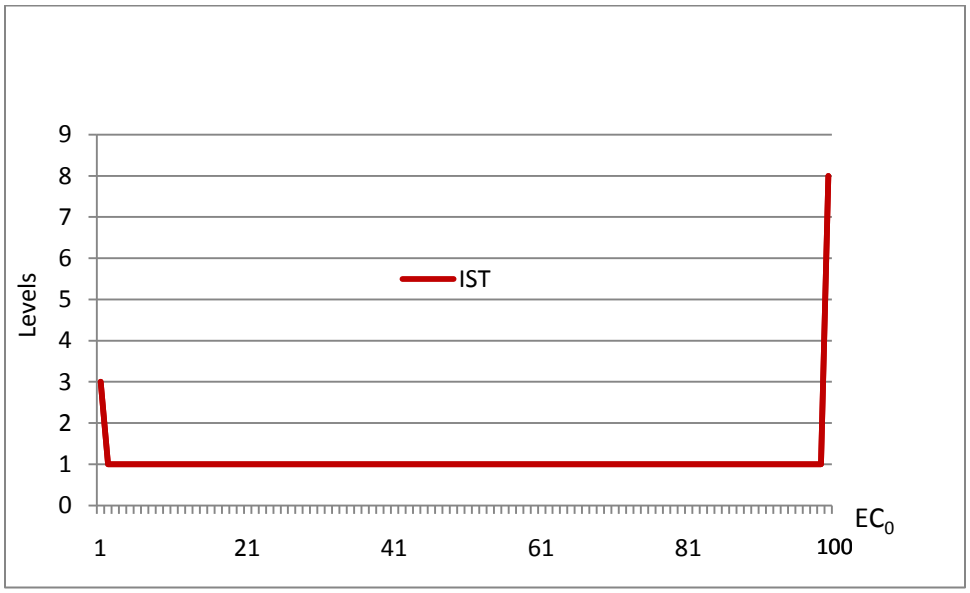

Figure 38: EC_o effect on IST Wind Pattern-1

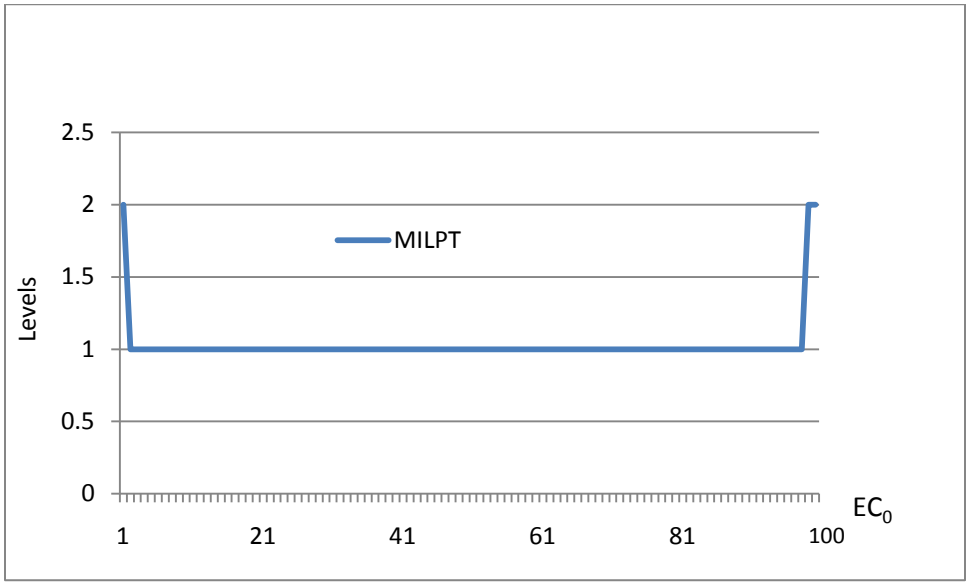

Figure 39: EC_o effect on MILPT Wind Pattern-2

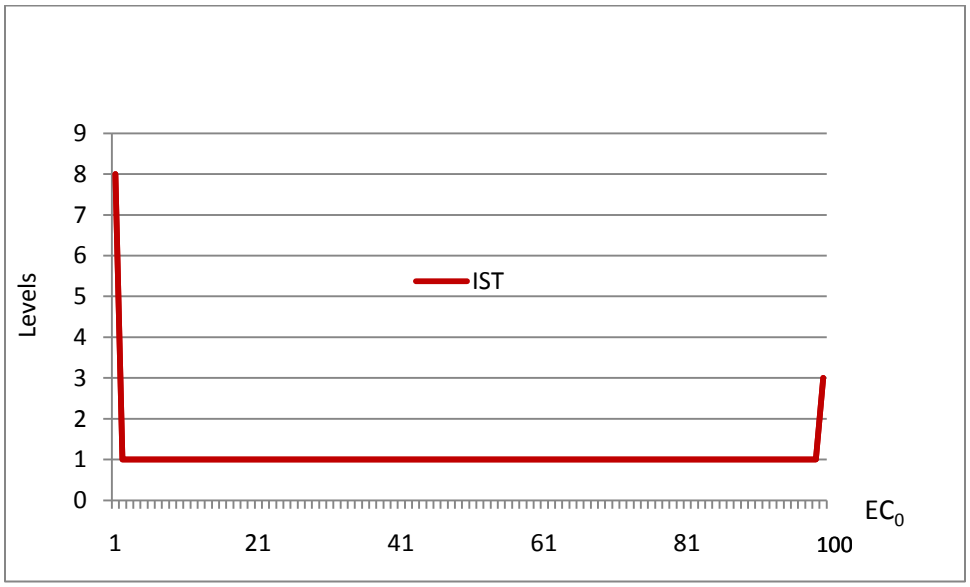

Figure 40: EC_o effect on IST Wind Pattern-2

5.7 CONCLUSIONS

Two algorithms that minimize the number of constant output power levels have been proposed and implemented. They have been tested on wind power data sets with 120 and 600 samples. Their analysis results have been presented. The role of initial energy in the supercapacitor on the number of levels in the output power was analyzed. From the results, it can be concluded that the initial energy of the supercapacitor should be kept at a value that is closer to 50% of the supercapacitor's capacity and this is found to minimize the number of $P_{ref\text{-}optimal}$ levels.

Therefore, when either of the Power Optimization Algorithms proposed in this chapter is used as the outer control loop with proposed topology of Chapter 3 as inner control loop, the short term wind power fluctuations can be eliminated effectively and quality of the power supplied into the grid can be improved.

CHAPTER 6

CONCLUSIONS

This thesis proposes the use of a Supercapacitor in tandem with a chopper and two layers of control systems to stabilize output power of a DFIG-WECS with an oscillatory input wind power. Figure 1 shows DFIG-WECS with proposed topology, the complete system.

The key contributions of this thesis are outlined chapter-wise:

Chapters 3 and 4

Chapter 3 proposes a Supercapacitor Energy Storage System that consists of a Supercapacitor, a buck-boost chopper and an inner control system. This topology receives an optimal DFIG output command ($P_{ref\text{-}optimal}$) from the optimization algorithm proposed in Chapter 5. The inner control system optimally controls the chopper such that power from Supercapacitor compensates changes in the input wind power and results in a constant DFIG output of $P_{ref\text{-}optimal}$. Therefore, it automatically controls the output of the DFIG using SESS to hold it at $P_{ref\text{-}optimal}$ despite an oscillatory wind power input at the turbine shaft. In Chapter 4, the performance of the proposed topology with the inner control loop is presented and discussed.

The most important practical benefit of this proposed solution is that the proposed solution can be implemented on any DFIG as an addition.

Chapter 5

In this chapter, two optimization algorithms are proposed. The objective of the optimization algorithms is to determine a minimum number of output power values for DFIG given a forecasted varying wind power input over a period 120 to 600 seconds. The optimization is constrained by limits of the DFIG and SESS. These optimization algorithms determine the least set of $P_{ref\text{-}optimal}$ values. As explained earlier, this set of $P_{ref\text{-}optimal}$ values are given to SESS such that the inner control loop can hold the DFIG's output to these values.

The key features of the topology proposed are:

- Decoupled design and control to ensure proposed topology integration into DFIG-WECS without any change in the DFIG-WECS
- Power quality improvement by short term power fluctuations elimination
- Total energy supplied to the grid equals total energy extracted from wind
- POA and SESS with control system works with any number of data samples and provides optimal power reference level(s) and minimizes the changes in DFIG WECS output

REFERENCES

[1] C. Millais and S. Teske "Wind Force 12: A blueprint to achieve 12% of the worlds electricity from wind power by 2020.", Greenpeace and European Wind Energy Association,www.ewea.org/03publications/WindForce12.htm, May, 2004.

[2] Chad Abbey and Géza Joos. "Short-term Energy Storage for Wind Energy Applications", 0-7803-9208-6/05© 2005 IEEE

[3] Van Der Hoven I. Power spectrum of horizontal wind speed in the frequency range from 0•007 to 900 cycles per hour, Journal of Meteorology 1957; 14: 160–164.

[4] Rohatgi JS, Nelson V. Wind Characteristics—an Analysis for the Generation of Wind Power. Alternate Energy Institute, West Texas A&M University: Canyon, TX, 1994;

[5] C. Luo, H. Banakar, B. Shen and B. Ooi, "Strategies to smooth wind power fluctuations of wind turbine generator, "IEEE Transactions on Energy conversion, vol. 22, pp. 341-349, June, 2007.

[6] W. Li, G. Joos, C. Abbey, " Wind power impact on system frequency deviation and an ESS based power filtering algorithm solution", Power systems conference and Exposition, PSCE, '06, pp.2077-2084, 2006.

[7] Chong Han, Alex Q, Haung, Ding Li, Haresh Mamath, Mike Ingram & Anley Atcityy, "Modeling & design of a transmission of Ultracap integrating voltage source converter with Ultracapacitor energy storage", Applied power electronics conference and exposition, APEC'01, pp.7-14,2006.

[8] Jiancheng Zhang, "Research on Supercapacitor energy storage system power networks", power electronics and Drives systems, vol. 4, pp1366-1369, 2005.

[9] Domenico Casadei, Gabriele Grandi and Cloudio Rossi, "A Supercapacitor based power conditioning system for power quality improvement and uninterruptible power supply", Industrial Electronics, vol.4, pp. 1247-1252,2002.

[10] I. Galkin, A. Stepanov and J. Laugis, "Outlook of usage of Supercapacitors in uninterruptable power supplies", Baltic Electronics Conference, pp 1-4, 2006.

[11] C. Banos, M. Aten, P. Cartwright and T.C. Green, "Benefits and control of STATCOM with energy storage in wind power generation", AC and DC Power Transmission", pp.230-235, 2006

[12] Chad Abbey, Geza Joos, "Supercapacitor Energy Storage for Wind Energy Applications", IEEE TRANSACTIONS ON INDUSTRY APPLICATIONS, VOL. 43, NO 3, MAY/JUNE, 2007

[13] F. Zhou, Chad Abbey, Geza Joos, L. Jiao and B.T. Ooi,"use of large capacity SMES to improve the power quality and stability of wind farms", Power Engineering Society General Meeting IEEE, vol. 2, pp. 2025-2030, June 2004.

[14] H.Ibrahim a. b, A.Ilinca, ,J.Perron, "Energy storage systems Characteristics and Comparisons", Renewable and Sustainable Energy Reviews 12 (2008) 1221–1250

[15] Document#10073627," Ultracapacitor Sizing", Maxwell Technologies, www.maxwell.com

[16] Andrew Stepanov, Ilija Galkin and Lauris Bisenieks, "Implementation of Supercapacitors in Uninterruptable power supplies", European conference of Power electronics and applications, vol.1-10, pp.4949-4955, 2007

[17] Wei Li and Geza Joos, "A Power Electronic Interface for a Battery Supercapacitor Hybrid Energy Storage System for Wind Applications", 39th IEEE PESC, vol. 1-10, pp. 1762-1768, 2008

[18] www.electronicsweekly.com/Articles/2006/03/03/37810/Supercapacitors-see-growth-as-costs-fall.htm

[19] Theodore Wildi, "Electrical Machines, Drives and Power Systems", publisher Prentice Hall, 2006

[20] Brendan Fox [et al], Wind power integration, connection and operational aspects, publisher, London Institution of Engineering and Technology, 2007

[21] http://www.energy.iastate.edu/renewable/wind/wem/images/wem-07_fig01.gif

[22] Istvan Erlich and Fekadu Shewarega, "Introduction of Wind Power Generation into the First Course in Power Systems", IEEE, 2007.

[23] Bimal K. Bose, "Modern Power Electronics and AC Drives" publisher Prentice Hall, 2002

[24] M. H. Rashid, "Power Electronics Circuits, Devices, and Applications", publisher Pearson Prentice Hall, 2004

[25] http://prod.sandia.gov/techlib/access-control.cgi/2001/010765.pdf

[26] http://en.wikipedia.org/wiki/Electric_double-layer_capacitor

APPENDIX A: ITERATIVE SEARCH TECHNIQUE

IST Code

```
clear; clc;

%xxxxxxxxxxxxxxxxxxxxxxx Data xxxxxxxxxxxxxxxxxxxxxxxxx%

Prate   = 1.5e6;
PconN   = -0.75e6;   PconP = +0.75e6;
Escmin   = 0;      Escmax = +157.3e6;
Esci    =0; %157.3e6; 78.65e6 %

%xxxxxxxxxxxxxxxxxxxxxxxxxxxxxxxxxxxxxxxxxxxxxxxxxxxxxxxxxx%
% 120 samples

% Figure 39 Data
Wind=[10 9 10 9 8 10 9 7 8 6 8 6 9 10 11 10 9 10 11 10 9 7 8 10 9 10 8 9 8 7 9 8 9 9 9 9
10 9 10 8 10 11 10 8 6 9 6 8 8 9 10 9 7 6 8 9 8 9 7 8 6 8 9 10 11 10 10 11 10 9 10 9 11 10
9 7 7 8 10 11 9 8 7 10 8 9 6 8 6 9 7 8 10 9 10 9 10 10 9 8 10 10 9 7 8 6 9 6 8 7 8 9 8 9 9 8
7 8 7 8];

% Figure 39 Data
%Wind=[7 8 6 7 7 6 8 8 6 9 6 8 8 9 10 9 7 6 8 9 8 9 7 8 6 8 9 10 11 10 10 11 10 9 10 9 11
10 9 7 7 8 10 11 9 8 7 10 8 9 6 8 6 9 7 8 10 9 10 9 10 10 9 8 10 10 9 7 8 6 9 6 8 6 8 10 9
11 10 9 8 9 7 8 6 8 10 9 10 9 8 10 9 7 8 6 9 10 11 10 9 10 11 10 9 7 8 10 9 10 8 9 8 7 9 8
9 8 9 9 ];

c=numel(Wind);

for j=1:c
   PW(1,j)=0;
end

for j=1:c
   if(Wind(1,j)<6)
      PW(1,j)=0;
   elseif(Wind(1,j)==6)
      PW(1,j)=0.12e6;
```

```
    elseif(Wind(1,j)==7)
        PW(1,j)=0.2e6;
    elseif(Wind(1,j)==8)
        PW(1,j)=0.29e6;
    elseif(Wind(1,j)==9)
        PW(1,j)=0.41e6;
    elseif(Wind(1,j)==10)
        PW(1,j)=0.55e6;
    elseif(Wind(1,j)==11)
        PW(1,j)=0.73e6;
    elseif(Wind(1,j)==12)
        PW(1,j)=0.95e6;
    elseif(Wind(1,j)==13)
        PW(1,j)=1.21e6;
    else
        PW(1,j)=1.21e6;
    end
end

Pw=PW;
n1=numel(Pw);

Prefa=0;Pwt=0;
for j=1:n1
    Prefa=Prefa+Pw(1,j);
    Pwt=Pwt + Pw(1,j);
    Pwx(1,j)=Pwt;
end

    Prefb= Prefa/j;   Psci = Esci; Psc=Psci;
    Pscmin=Escmin; Pscmax=Escmax;

ctr=1; Pwd=0; PrefNew=0; Pwb=0;
 while(ctr<=n1)
%xxxxxxxxxxxxxxxxxxxxxxxxx Middle xxxxxxxxxxxxxxxxxxxxxxxxxxxxx%

      if(Pw(1,ctr)<Prefb)
        Pscn=Prefb-Pw(1,ctr);
         if (((Psc - Pscn)>=Pscmin) && (Pscn<=PconP) && (Prefb<=Prate))
            Pref(1,ctr)=Prefb;
            Pscd(1,ctr) = Psc - Pscn;
            Psc = Psc - Pscn;
```

```
        else
            b=ctr;
            Pwb=0;
            while(Pw(1,ctr)<Prefb)
                Pwb=Pwb+Pw(1,ctr);
                ctr=ctr+1;
                if(ctr>n1)
                    break;
                end
            end
            Pwb=Pwb/(ctr-b);
            if(Psci==Pscmin)
                Pwb = Pwb - (0.75 * Pwb);
                Prefb=Pwb;
            end
            ctr=ctr-1;
            for i=b:ctr
                Pscn=Pw(1,i)-Prefb;
                if (((Psc + Pscn)>=Pscmin) && (Pscn<=PconP) && (Prefb<=Prate))
                    Pref(1,i)=Prefb;
                    Pscd(1,i) = Psc + Pscn;
                    Psc = Psc + Pscn;
                end
            end
            Pwd=0;
            if(ctr==n1)
                ctr=ctr-1;
            end
            for j=1:ctr
                Pwd=Pwd+Pref(1,j);
            end
            PrefNew=(Pwt-Pwd)/(n1-ctr);
            Prefb=PrefNew;
        end
    else                % Pw > Pref
        Pscn=Pw(1,ctr)-Prefb;
        if (((Psc + Pscn)<=Pscmax) && (Pscn<=PconP) && (Prefb<=Prate))
            Pref(1,ctr)=Prefb;
            Pscd(1,ctr) = Psc + Pscn;
            Psc = Psc + Pscn;
        else
            b=ctr;
```

```
            Pwb=0;
            while(Pw(1,ctr)>Prefb)
                Pwb=Pwb+Pw(1,ctr);
                ctr=ctr+1;
                c=ctr;
                if(ctr>n1)
                    break;
                end
            end
            Pwb=Pwb/(ctr-b);
            if(Psci==Pscmax)
                Pwb = Pwb + (0.75 * Pwb);
                Prefb=Pwb;
            end
            ctr=ctr-1;
            for i=b:ctr
                Pscn=Pw(1,i)-Prefb;
                if (((Psc + Pscn)<=Pscmax) && (Pscn<=PconP) && (Prefb<=Prate))
                    Pref(1,i)=Prefb;
                    Pscd(1,i) = Psc + Pscn;
                    Psc = Psc + Pscn;
                end
            end
            Pwd=0;
            if(ctr==n1)
                ctr=ctr-1;
            end
            for j=1:ctr
                Pwd=Pwd+Pref(1,j);
            end
                PrefNew=(Pwt-Pwd)/(n1-ctr);
                Prefb=PrefNew;
        end
    end
    ctr=ctr+1;
end

Pot=0;Pct=0;
for q=1:n1
    Pot=Pot+Pref(1,q);
    Pod(1,q)=Pot;
    Pa=Pw(1,q)-Pref(1,q);
```

```
  Pc(1,q)=Pw(1,q)-Pref(1,q);
  Pct=Pct+Pc(1,q);
 end

Pref'
Pwt
Pot

  subplot(2,1,1)
  plot(Pw,'.-b');   % Power gen or WT
  hold on
  grid on
  plot(Pref,'.r');  % P reference
  xlabel('sec');
  ylabel('Power');
  title('Pref Optimal')
  hold off
  subplot(2,1,2)
  plot(Pwx,'.b');   % Power gen or WT
  hold on
  plot(Pod,'.r');   % Power gen or WT
  hold on
  xlabel('sec');
  ylabel('Power');
  title('Pref Optimal')
```

IST Results

120 Data Samples

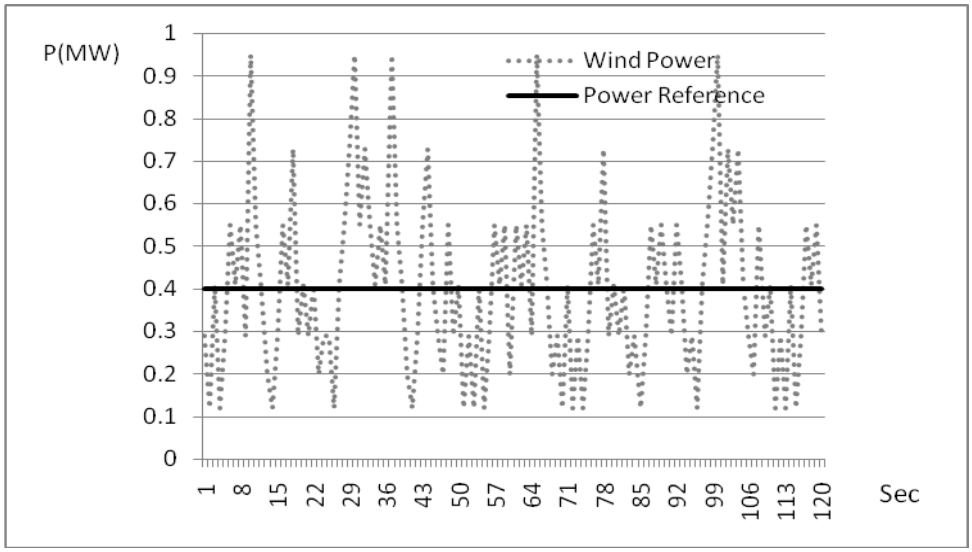

Figure 41: Pw and Pref for IST (120 Samples)

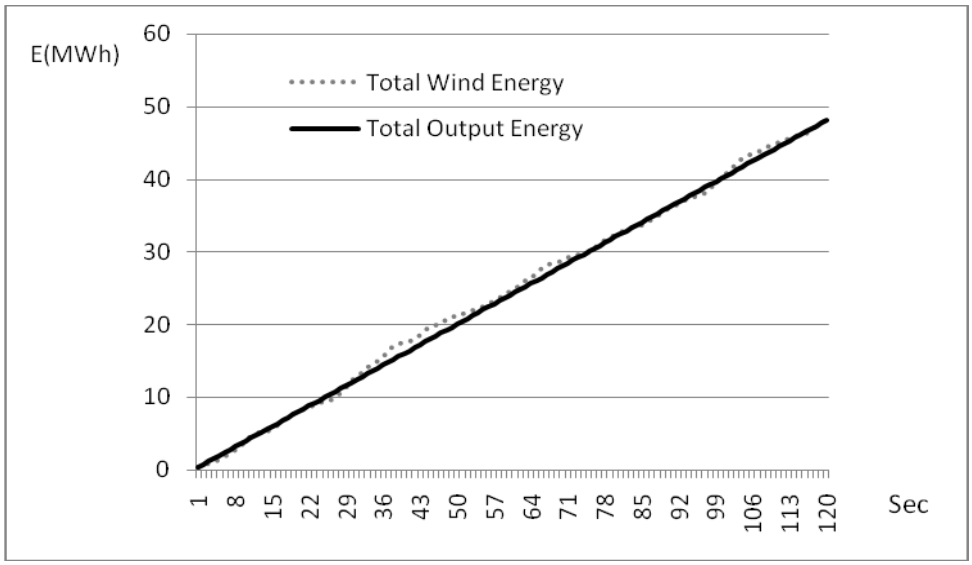

Figure 42: Total wind and IST Energy (120 Samples)

600 Data Samples

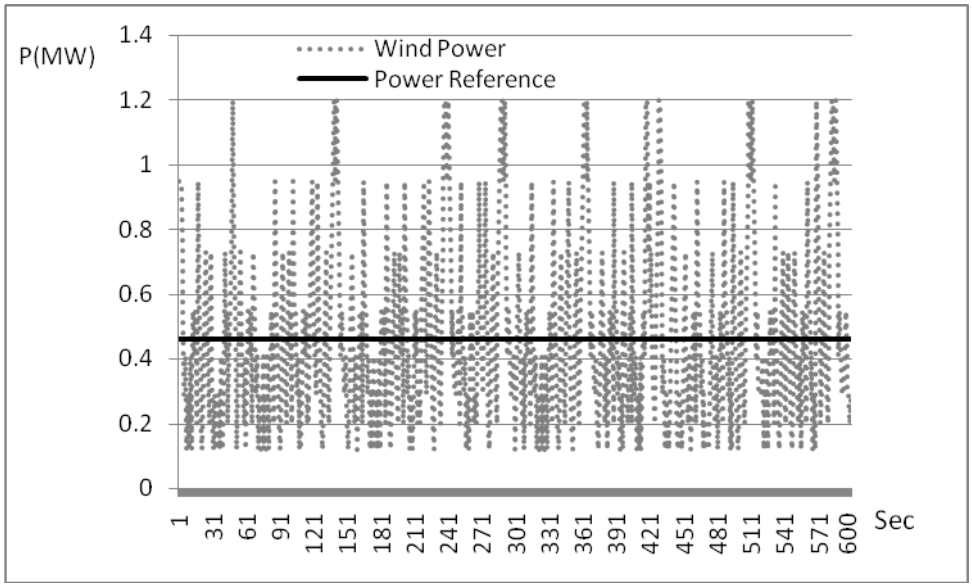

Figure 43: Pw and Pref for IST 600 Samples

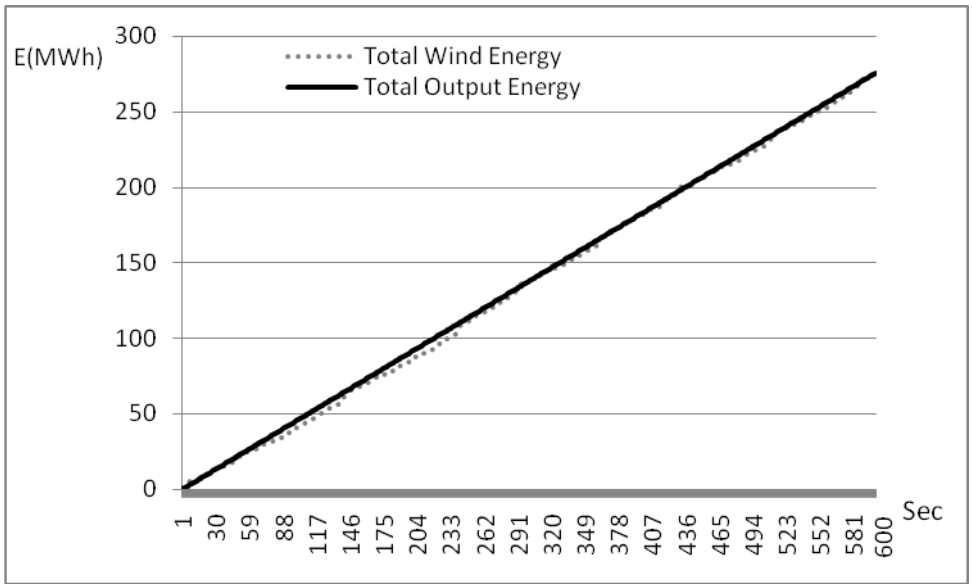

Figure 44: Total wind and IST Energy (600 Samples)

APPENDIX B: MIXED INTEGER LINEAR PROGRAMMING TECHNIQUE

MILPT Code

```
close all; clear all;  clc;    clear prob;

%      ------------DATA------------------
Pomax   = +1.5e6;
Pcmin   = -0.75e6;   Pcmax = +0.75e6;
Ecmin   = 0;      Ecmax = +187.2e6;
Ec0     =78.65e6;

% 120 Samples (Wind Pattern)
 Wind=[8 6 9 6 8 10 9 10 8 12 10 9 7 6 8 10 9 11 8 9 8 9 7 8 8 6 9 10 11 12 10 11 10 9 10
9 12 10 9 7 6 8 10 11 9 8 7 10 8 9 6 8 6 9 6 8 10 9 10 7 10 9 10 8 12 10 9 7 8 6 9 6 8 6 8
10 9 11 8 9 8 9 7 8 6 8 10 9 10 9 8 10 9 7 8 6 9 10 11 12  9 11 10 11 9 8 7 10 8 9 6 8 6 9 6
8 10 9 10 8];

 c=numel(Wind);

 % blank 120 Samples storage created
for j=1:c
   Pw(1,j)=0;
end

% MPPT based corresPonding Power stored for 120 wind samples
for j=1:c
   %Wind(1,j)=Wind(1,j);
   if(Wind(1,j)<6)
      Pw(1,j)=0;
   elseif(Wind(1,j)==6)
      Pw(1,j)=0.12e6;
   elseif(Wind(1,j)==7)
      Pw(1,j)=0.2e6;
   elseif(Wind(1,j)==8)
      Pw(1,j)=0.29e6;
```

```
    elseif(Wind(1,j)==9)
        Pw(1,j)=0.41e6;
    elseif(Wind(1,j)==10)
        Pw(1,j)=0.55e6;
    elseif(Wind(1,j)==11)
        Pw(1,j)=0.73e6;
    elseif(Wind(1,j)==12)
        Pw(1,j)=0.95e6;
    elseif(Wind(1,j)==13)
        Pw(1,j)=1.21e6;
    else
        Pw(1,j)=1.21e6;
    end
end
  Pw=Pw';

%      -----------DATA END --------------

Nh = numel(Pw); Nh1 = Nh - 1;

Nr = 1 + 3 * Nh + 2 * Nh1 ;

Nc = 4 * Nh ;

prob.a  = sparse(Nr , Nc );
prob.blx (0*Nh+1:1*Nh,1)    = Pcmin;       prob.bux(0*Nh+1:1*Nh,1) = Pcmax;
prob.blx (1*Nh+1:2*Nh,1)    = 0;           prob.bux(1*Nh+1:2*Nh,1) = Pomax;
prob.blx (2*Nh+1:4*Nh,1)    = 0;           prob.bux(2*Nh+1:4*Nh,1) = 1;

Pwt=0;
for i=1:Nh
    Pwt=Pwt+Pw(i,1);
    Pwd(i,1)=Pwt;
end

%   sum (Pct) = 0;
Rw  = 0;
prob.a(Rw+1,1:Nh) = 1;     prob.blc(Rw+1) = 0; prob.buc(Rw+1) = 0;

%   Ecmin - Ec0 < sum_k(Pck) <  Ecmax - Ec0
Rw = 1;
prob.blc (Rw+(1:Nh)) = Ecmin - Ec0;     prob.buc (Rw+(1:Nh)) = Ecmax - Ec0;
```

```
for t = 1 : Nh; for k  = 1:t;   prob.a(Rw+t,1:k) = 1;   end;    end;

% Pwt < Pct + Pot  <   Pwt
Rw = 1 + Nh;
prob.blc(Rw + (1:Nh)) = Pw;     prob.buc(Rw + (1:Nh)) = Pw;
prob.a(Rw + (1:Nh) ,      (1:Nh)) = speye(Nh);     %Pc
prob.a(Rw + (1:Nh) , Nh + (1:Nh)) = speye(Nh);     %Po


% -inf < Pot+1 - Pot - Pomax * USt+1   < 0
Rw = 1 + 2*Nh;
prob.blc(Rw + (1:Nh1)) = -inf;      prob.buc(Rw + (1:Nh1)) = 0;
prob.a  (Rw + (1:Nh1),  Nh+(1:Nh1) ) = -speye(Nh1);            %Pot
prob.a  (Rw + (1:Nh1),  Nh+(2:Nh ) ) = ...
prob.a  (Rw + (1:Nh1),  Nh+(2:Nh ) )   +speye(Nh1);            %Pot+1
prob.a  (Rw + (1:Nh1),2*Nh+(2:Nh ) ) = -speye(Nh1) * Pomax;     %USt1

% 0    < Pos,t+1 - Pos1 + Pomax * Ds,t+1  < inf
Rw = 1 + 2*Nh + Nh1;
prob.blc(Rw + (1:Nh1)) = 0;      prob.buc(Rw + (1:Nh1)) = inf;
prob.a  (Rw + (1:Nh1),  Nh+(1:Nh1) ) = -speye(Nh1);    %Pot
prob.a  (Rw + (1:Nh1),  Nh+(2:Nh ) ) = ...
prob.a  (Rw + (1:Nh1),  Nh+(2:Nh ) )   +speye(Nh1); %Pot+1
prob.a  (Rw + (1:Nh1),3*Nh+(2:Nh ) ) = +speye(Nh1) * Pomax;    %UDt+1

% 0    <  Us,t+1 - Us,t  - Ss,t+1 + Ds,t+1 < 0
% 0 < Sst + Dst  <   1
Rw = 1 + 2*Nh + 2*Nh1
prob.blc(Rw + (1:Nh)) = 0;      prob.buc(Rw + (1:Nh)) = 1;
prob.a  (Rw + (1:Nh), 2*Nh+(1:Nh) ) = speye(Nh) ;    %Sst
prob.a  (Rw + (1:Nh), 3*Nh+(1:Nh) ) = speye(Nh) ;    %Dst

prob.c(1,Nc) = 0;
prob.c(2*Nh + (1:2*Nh) ) = 1;

prob.ints.sub=[2*Nh + (1:2*Nh)];

[r, res]=mosekopt('minimize',prob);

Pc = res.sol.int.xx(0*Nh+1:1*Nh);
Po = res.sol.int.xx(1*Nh+1:2*Nh);
S  = res.sol.int.xx(2*Nh+1:3*Nh);
```

```
D  = res.sol.int.xx(3*Nh+1:4*Nh);
Ec = prob.a(2:Nh+1,:) * res.sol.int.xx;

Pot=0;
for i=1:Nh
    Pot=Pot+Po(i,1);
    Pod(i,1)=Pot;
end
 ['    Pw        Pc       Ec          Po         S         D ']
[Pw Pc Ec Po S D]
Pwt
Pot
   subplot(2,1,1)
   plot(Pw,'.-b');
   hold on
   grid on
   plot(Po,'.r');
   xlabel('Sec');
   ylabel('Power');
   title('Mosek Pref Optimal')
   hold off

   subplot(2,1,2)
   plot(Pwd,'.b');
   hold on
   plot(Pod,'.r');
   hold on
   xlabel('Sec');
   ylabel('Power');
   title('Pref Optimal')
   hold off
```

120 Data Samples

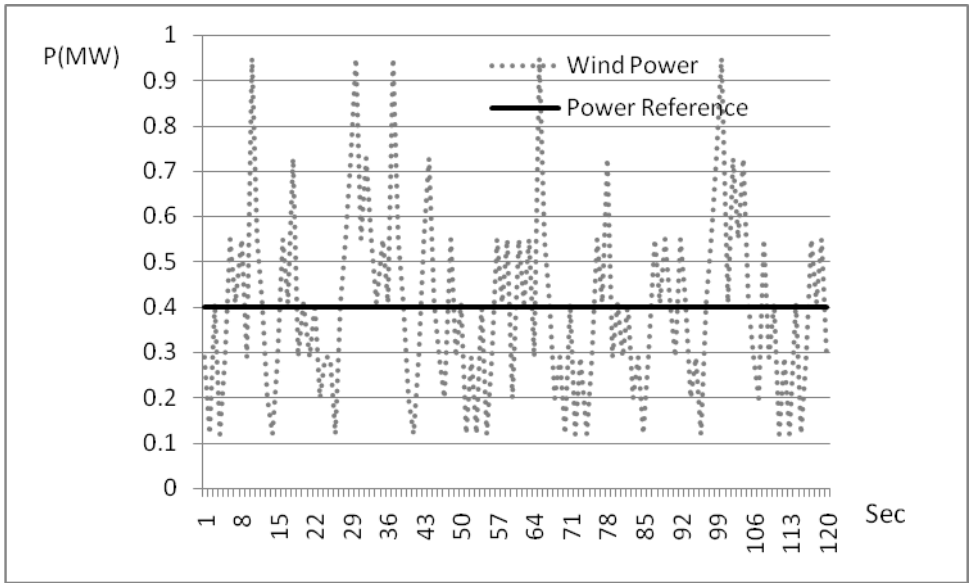

Figure 45: Pw and Pref for MILPT 120 Samples

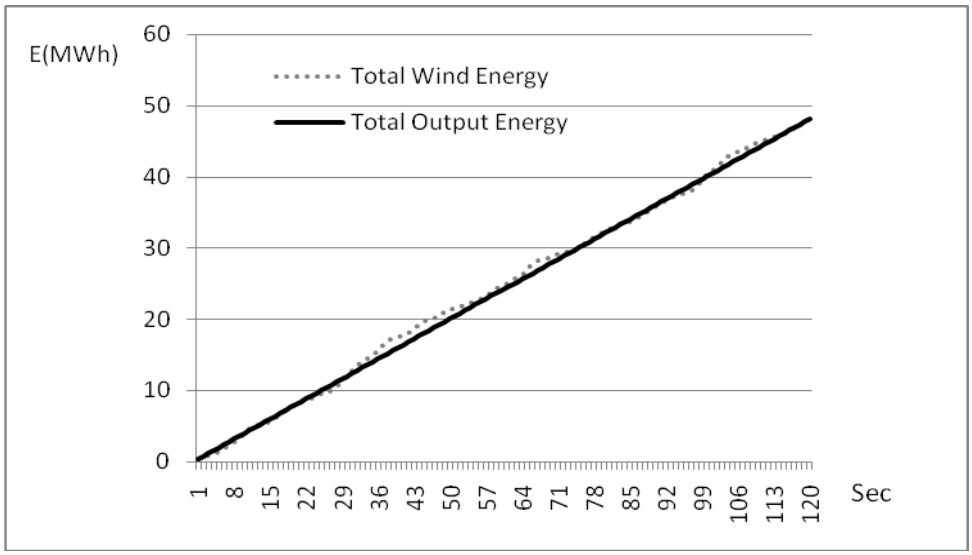

Figure 46: Total wind and MILPT Energy (120 Samples)

600 Data Samples

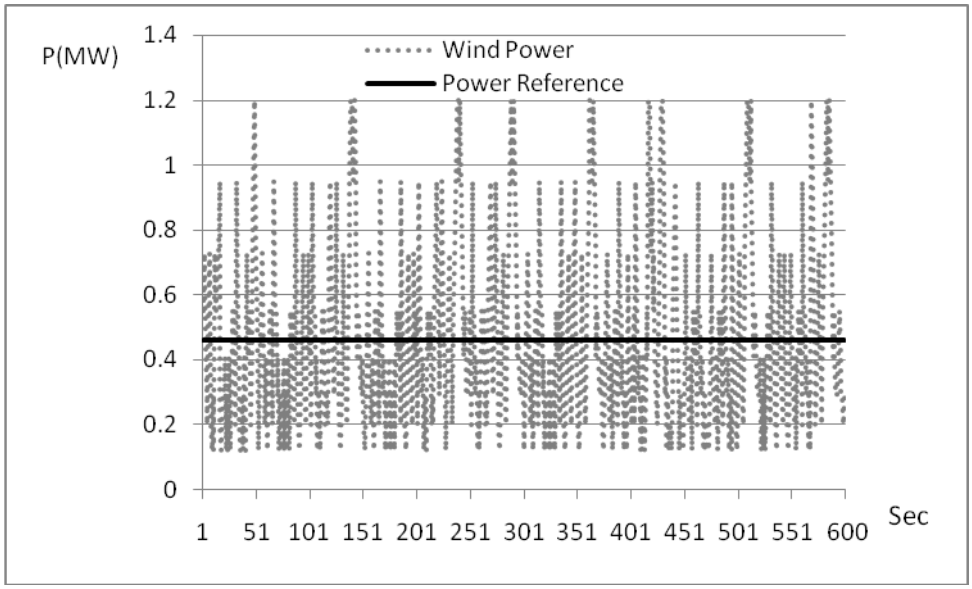

Figure 47: Pw and Pref for MILPT 600 Samples

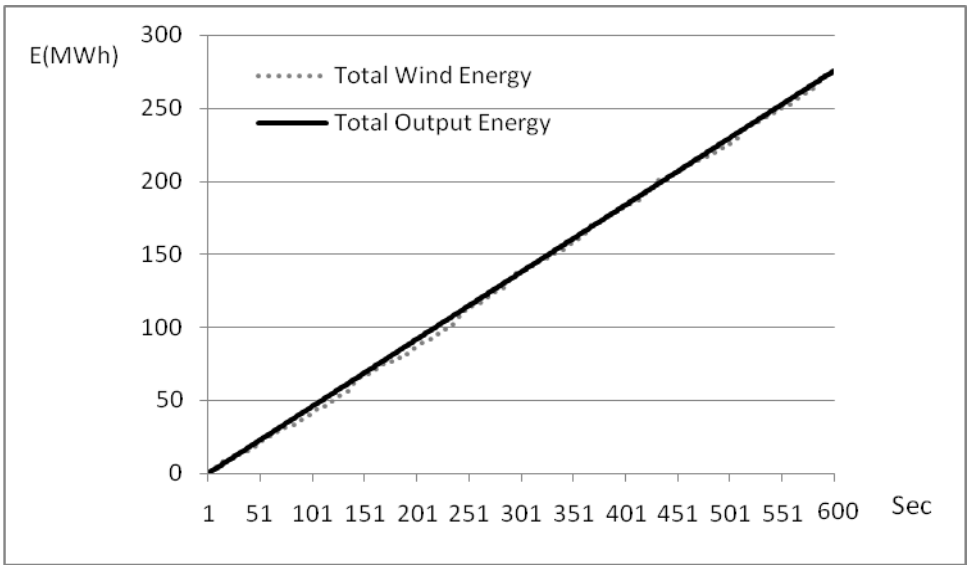

Figure 48: Total wind and MILPT Energy (600 Samples)

120 Data Samples with zero, rated and above rated wind speeds

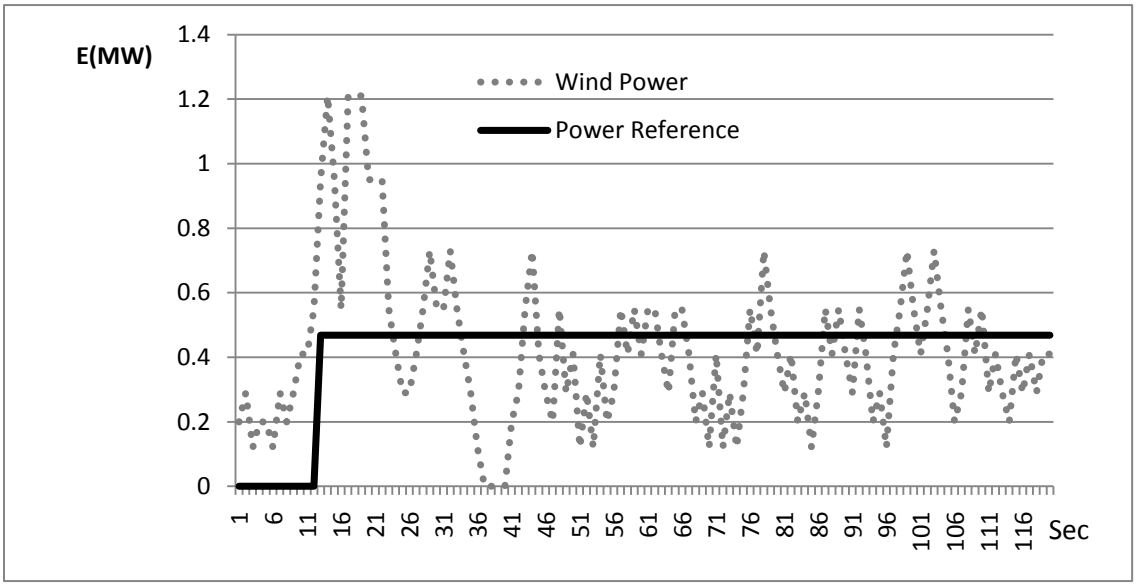

Figure 49: Pw and Pref for MILPT 120 Samples

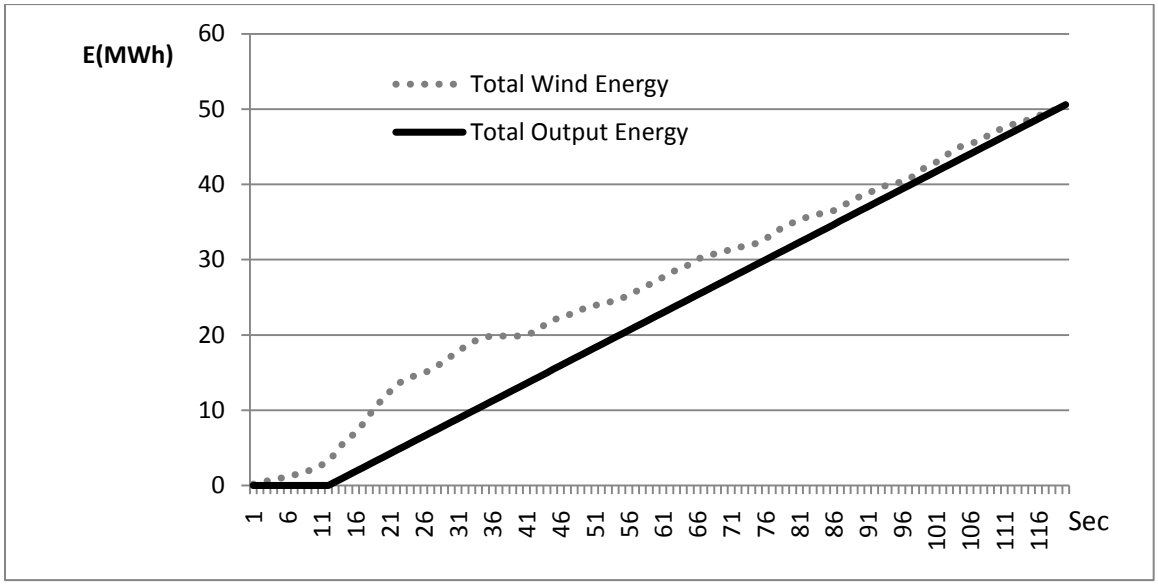

Figure 50: Total wind and MILPT Energy (120 Samples)

APPENDIX C: SIMULATED SYSTEM DATA

Table 2: Induction machine data

Name	Value	Name	Value
f_s	60 Hz	H	5.041 s
V_{nom}	575 V(L-L)	F	0.01 pu
P_{nom}	1.5e6/0.9 VA	P	3-pairs
R_s	0.00706 pu	R_r	0.005 pu
L_{ls}	0.171 pu	L_{lr}	0.156 pu
L_m	0.29		

Table 3: Turbine data

Name	Value	Name	Value
P_{mech}	1.5e6 W	ωr @ C	1.2 pu
P @ C	0.73 pu		

Table 4: Topology data

Name	Value	Name	Value
E_{sc}	157.3 MJ	C	150 F
V_{nom}	1200 V	V_{max}	1350 V
V_{min}	100 V	L	10 mH
R_{sc}	4.5 mΩ		

Table 5: Misc data

Name	Value	Name	Value
V_{dclink}	1200 V	$L\text{-}R_{lchoke}$	0.30 pu
C_{dclink}	10e-3 F	f_{pwm}	1620 Hz
$R\text{-}R_{lchoke}$	0.0030 pu		